

UNCLASSIFIED

AD 406 842

DEFENSE DOCUMENTATION CENTER

FOR

SCIENTIFIC AND TECHNICAL INFORMATION

CAMERON STATION, ALEXANDRIA, VIRGINIA



UNCLASSIFIED

NOTICE: When government or other drawings, specifications or other data are used for any purpose other than in connection with a definitely related government procurement operation, the U. S. Government thereby incurs no responsibility, nor any obligation whatsoever; and the fact that the Government may have formulated, furnished, or in any way supplied the said drawings, specifications, or other data is not to be regarded by implication or otherwise as in any manner licensing the holder or any other person or corporation, or conveying any rights or permission to manufacture, use or sell any patented invention that may in any way be related thereto.

63-4-1

NAVWEPS REPORT 8353
NOTS TP 3240
COPY 52

RECEIVED BY DDC

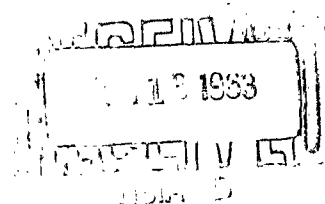
AS AD No. 406842

406 842

DESIGN CRITERIA FOR LARGE ACCURATE SOLID-PROPELLANT STATIC-THRUST STANDS

by

D. P. Ankeney and C. E. Woods
Test Department



ABSTRACT. This report presents design criteria for the construction of a large solid-propellant static-thrust stand to meet specific requirements of accuracy, flexibility, adaptability, ease of assembly and operation, safety, and low cost. Design concepts of dynamic stand evaluation, calibration accuracy and error analysis, continuous-mass measurement, in-place calibration, alignment, damage control, and environmental testing are discussed. Also included in the report is a suggested design procedure formulated to provide guidance in the design and development of a static-test stand that will attain the unique goals of a particular facility. This report supersedes IDP 1551 of the same title, dated December 1962.

Released to ASTIA for further dissemination with
out limitations beyond those imposed by security
regulations.



U. S. NAVAL ORDNANCE TEST STATION

China Lake, California

June 1963

U. S. NAVAL ORDNANCE TEST STATION

AN ACTIVITY OF THE BUREAU OF NAVAL WEAPONS

C. BLENNAN, JR., CAPT., USN
Commander

WM. B. MCLEAN, PH.D.
Technical Director

FOREWORD

The design of large solid-propellant static-thrust stands for testing rocket motors has become increasingly complex with the requirements for the measurement of all six components of force to an accuracy of 1.0% or better. When the need to simulate flight environmental conditions is also added, the problems facing the designer are multiplied and, in some cases, conflicting in solution.

This report, written for personnel in the fields of test-facility design and development, describes some of the problems inherent in static test-stand design and suggests solutions. These suggested solutions are based on five years of experience in the design and development of a large thrust-stand facility at the U. S. Naval Ordnance Test Station, China Lake, California. The work involved both the development of a facility capable of accurately evaluating large motors and the determination of new test techniques and facility capabilities. It was funded by Bureau of Weapons Task Assignments SP-271-17-59, SP-271-17-60, SP-271-22-60, and SP-71402-8.

This report, which supersedes IDP 1551 of the same title, dated December 1962, has been reviewed for technical accuracy by W. F. Thorn and R. W. Murphy.

Released under
the authority of
IVAR E. HIGHBERG
Head, Test Department

R. A. APPLETON
Head, Range Division

NOTS Technical Publication 3240
NAVWEPS Report 8353

Published by Test Department
Manuscript 30/MS-578
Supersedes IDP 1551
Collation Cover, 25 leaves, abstract cards
First printing 285 numbered copies

CONTENTS

Introduction.	1
Facility Design and Operation	1
Ramifications of the 0.1% Accuracy Requirement.	2
0.1% Single-Component Stand Has Six-Component Stand Complexity.	4
The Thrust Stand as a Force-Vector System	5
Initial Stand Alignment	8
Ease of Assembly and Disassembly.	9
Modular Concept	10
Damage Control.	12
Ease of Load Cell Calibration	13
Environmental Control	18
Mass Measurement.	20
Thrust Stand Design Procedure	26
Appendixes:	
A. Thrust Stand Goals.	28
B. Explanation of Necessity for Using Long Stand Members	30
C. Four Bar Linkage Analysis	36
D. Flexure Analysis.	41
References.	47

Figures:

1. Natural Stand Frequencies Versus Motor Weight.	3
2. Effect of Geometric Size on Natural Frequency.	3
3. Six-Component Thrust Stand Configuration	6
4. Four-Bar Linkage Stand With Thrust Takeout Flexibility	7
5. Stand Alignment Instrumentation Array.	9
6. Typical Flanged Joint Load-Deflection Curve.	11
7. Improved Linear Joint Load-Deflection Curve.	11
8. Load-Cell Trace From Single Component Stand With Nonlinear Spring Curve	16
9. Load-Cell Trace From Three-Component Stand With Improved Spring Curve	17
10. Data Combination Correction Procedure.	21
11. Calculation for Mass Measurement Showing Schematic of Motor With Servo Shaker at Natural Frequency	21
12. Schematic Diagram of Mass Measuring System	22
13. Rocket Motor and Stand Displacement as a Function of Frequency (Live Rocket Motor).	24
14. Rocket Motor and Stand Displacement as a Function of Frequency (Burnt Rocket Motor)	24
15. Vibrating Mass as a Function of Burning Time	26

INTRODUCTION

The design complexity of mechanical systems such as thrust stands is largely dictated by the goals toward which the specific design is aimed. The need for higher accuracy, increased frequency response, etc., invariably results in greater design sophistication. Unfortunately, this higher degree of sophistication can be attained only at the expense of increasing costs in both thrust-stand hardware and in thrust-stand setup time. To fire motors so as to obtain increasingly accurate data requires an ever-pyramiding facility in both instrumentation and data reduction as well as more extensively trained operations personnel. To accomplish production firings on schedule at minimum cost and yet produce highly-accurate data, calls for an extensive, well-trained, and integrated group of specialists. These can be produced only as a result of years of operating experience in trying to meet stringent data requirements in the field of thrust-stand testing.

In addition to trained personnel, there is a continuing need for equipment maintenance and repair in order to assure system operability and accuracy; however, the time and money for upkeep are often grudgingly spent. Thus, it is sometimes questionable as to whether system maintenance is keeping up with the rate at which the equipment goes out of repair and calibration. These problems are compounded by the continually-changing test conditions which make even more difficult the necessary, but time-consuming, maintenance and calibration of equipment.

FACILITY DESIGN AND OPERATION

The requirements for an accurate thrust-stand facility must first be defined before going into actual design. These requirements are not always easy to interpret since they contain many conflicting factors.

The thrust-stand design program began at NOTS in 1958. At that time, specific facility requirements were determined only after an intensive study had been made by local motor-development people. These requirements, of which only a small part pertains to thrust-stand design per se (Appendix A), were quite extensive. Although the primary purpose of this report is to discuss the problems of large motor-thrust-stand design, it must be emphasized that, in the final analysis, facility instrument requirements are the first order of import. Without the ability to transmit and reduce data signals to fractions of a percent, the best thrust stand in the world will be of little practical value. The stand is only the first of many factors which will contribute small, but compounding errors to the final data. Then, too, with test-stand operation

comes the increasing desire for closer test scheduling, lower test costs, and safer operating conditions. All of this tends to erode the time-consuming procedures needed to maintain accuracy. Consequently, thrust-stand operation requirements become an integral and correlated part of the overall design requirements.

To meet facility design and operation requirements, the following goals must be attained:

1. 0.1% accuracy
2. Six-component measurement
3. High-frequency response (stand linearity)
4. Ease of assembly and disassembly
5. Ease of stand alignment
6. Damage control
7. Ease of load-cell calibration
8. Environmental control (temperature conditioning, high-altitude simulation)
9. Continuous mass measurement

This report describes the design criteria for thrust-stand construction to meet the above goals and shows how these design, operation, and control features are interrelated. In fact, they are so interrelated that a discussion item by item is difficult. Therefore, this discussion will present the interrelationships in a logical order of development.

RAMIFICATIONS OF THE 0.1% ACCURACY REQUIREMENT

The first reaction of many people when they see the figure of 0.1% stand accuracy is to vigorously maintain that only an accuracy of 1% or 2% is actually needed. However, it is pointed out that by the time the final data from the data system beyond the stand is reduced this accuracy figure may actually have deteriorated to anywhere between 1% and 5%. It must also be realized that if we can build stands having an accuracy of 0.1% then we can certainly build a stand accurate to 1%. In other words, if we can't demonstrate the knowhow to design a stand capable of operating at an accuracy of 0.1%, then we cannot guarantee a stand accuracy of 1%.

The first consideration in large motor-thrust-stand design is the relative softness or flexibility of the motor and motor-stand support members. Under thrust, stand deflections in the region of tenths of inches are common. Also, motor-case diametral expansion and change in length under burning pressure are often greater than the stand deflections. Larger motor-case expansions occur with more highly stressed motor cases. One interesting aspect of stand flexibility is the effect it has on the natural frequency of various size stands. Historically,

this is the first important characteristic we stumbled upon during the design program at NOTS. Information gleaned from a search of the early literature in this field is shown in Fig. 1. Figure 2 further emphasizes how increased stand sizes decrease the natural frequency of the stands making it very difficult to build a high-frequency response stand for large rocket motors. The lower natural frequencies of larger stands mean that larger deflections under thrust will occur. This in turn means that there will be a tendency for the motor supports to absorb thrust in deflection and this portion of the thrust will not be measured, thus creating small errors.

$f_n = \frac{1}{2\pi} \sqrt{\frac{K}{M}}$ $f_n = \text{NATURAL FREQUENCY (CYCLES/SECOND)}$		
PUBLISHED RESULTS FROM LITERATURE SURVEY		
WT OF MOTOR	f_n - NATURAL FREQUENCY	SOURCE
3.2 LB	2,600 CPS	ROHM & HAAS CO.
20 LB	1,400 CPS	ROHM & HAAS CO.
1,000 LB	500 CPS	BALDWIN-LIMA-HAMILTON CO.
20,000 LB	25 CPS	AEROJET
RESULTS OF STUDY INTO AXIAL THRUST ACCURACY		

FIG. 1. Natural Stand Frequencies Versus Motor Weight.

Increasing dimensions by "n" causes natural frequency to decrease by 1/n.

Based on scale relationships and previous studies, the best " f_n " for a 20,000 lb. motor stand is 180 cps.

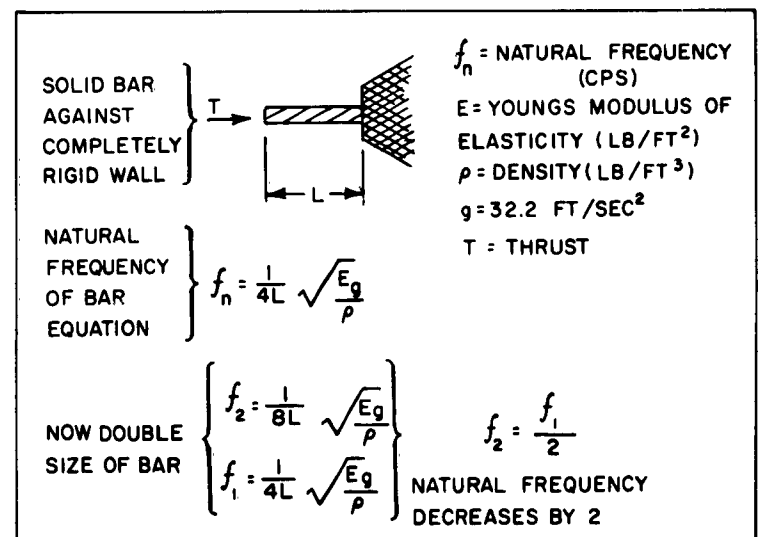


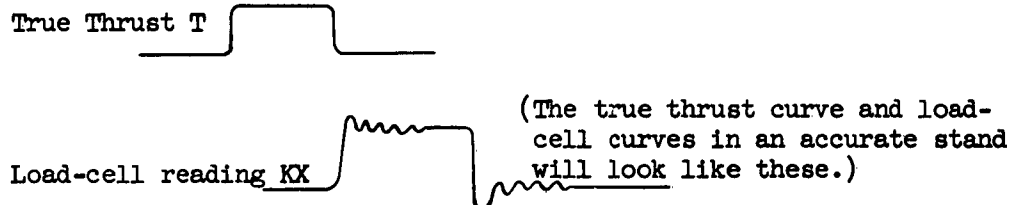
FIG. 2. Effect of Geometric Size on Natural Frequency.

0.1% SINGLE-COMPONENT STAND HAS SIX-COMPONENT STAND COMPLEXITY

If a single-component stand is designed for 0.1% accuracy, the design of the side members of the stand will often approach the six-component requirements. The following calculations illustrate this:

(Thrust) x (Permissible Error) = (100,000 lb) (0.001) = 100 lb. Therefore, it is apparent that 100 lb is the maximum total allowable restraint or friction in stand supports.

Now a 20-cps stand frequency is typical for large motors in the 20,000-lb weight range.



$$f = \frac{1}{2\pi} \sqrt{\frac{K}{M}}$$

$$K = (2\pi f)^2 M$$

$$T = KX; X = \frac{T}{K} = \frac{T}{(2\pi f)^2 M}$$

K = spring constant of main thrust takeout assembly, lb/ft.

X = deflection of center of gravity of stand-motor combination, ft.

f = natural frequency, cps.

$$X = \frac{(100,000)}{(2\pi)^2 (20)^2 \frac{20,000}{32.2}} = 0.01014 \text{ ft} = 0.122 \text{ inch}$$

To compensate for hard starts use a dynamic-load factor of 2. Stand will deflect X = 0.122 inch under steady-state loads and, under hard starts, may deflect as much as X_{hard start} ≈ 0.244 inch. The stand support members must not resist the 0.122- to 0.244-inch motion of the stand by more than 100 lb. Or, restated, the total resistance to this stand motion due to friction and bending in flexure of the support mechanisms must be less than 100 lb. This equates, for a 20,000-lb motor mounted on rollers, to a friction coefficient of 0.005. For a rotating ball bearing (according to Ref. 1) a friction coefficient of 0.001 might be a minimum. But the bearings in this thrust stand must start from a complete standstill and the starting friction coefficient could easily

be ten times 0.001 or $f = 0.010$, particularly if the bearings are not sealed or maintained on rolling or smooth surfaces. The conclusion is that the actual friction coefficient will be variable and, in any event, probably not predictable. Furthermore, the motor will experience at least some additional restraint from the side-stand restraining members due to the deflection caused by thrust and this will be added to the friction of the bearing support. Although it is possible to obtain bearings with double bearing rows in which the middle race can be rotated so as to maintain the friction coefficient at $f = 0.001$, this adds to the complexity and expense of the stand. At NOTS, after investigating the bearing application to thrust stand design, it was concluded that mounting the motor on legs with universal flexure pivots at each end of a specific leg (or side-support) member would be easier and less expensive. The flexure procedure produces essentially no friction since it involves bending a thin leaf of steel and, with the proper leg or side-support member length, it can easily be adapted so that the total retarding restraint is well within the 100-lb limit specified in the above example. Also, the restraint would be linear with deflection and would behave essentially like a spring in flexure which yields extremely reproducible results (see Ref. 2).

Now, here, we have a motor restrained by six to seven members consisting of individual bars with a universal flexure on each end of each bar. By placing a load cell in each member, a limited six-component stand is created. The word 'limited' is quite true since in such a converted single-component stand there has been no provision for alignment equipment or alignment-adjustment equipment and as a result it will probably perform poorly.

The length of the stand members needed to maintain this 0.1% accuracy can be calculated for any type of flexure used. A sample calculation is given in Appendix B to demonstrate why long-stand members are necessary.

THE THRUST STAND AS A FORCE-VECTOR SYSTEM

A practical thrust stand which approaches the 0.1% accuracy goal consists of members which contain the motor in the simplest possible manner to minimize costs in stand fabrication, motor assembly and alignment, and data reduction. One possible stand configuration (Fig. 3) consists of one existing stand which was converted to six-component capability by adding load cells to the four support legs. Since the existing motor-handling harness and fixtures were used in this stand as attach points, it does not represent the best configuration for accuracy and calibration. It would have been better to attach the front side-force member farther forward at the main thrust flexure-thrust cone joint.

Also, the trunion-block attachment on the handling harness wheels (ball bearings) represents a departure from flexured stand practice. In order to resist the possible six components of force and moment produced by a large motor, there will be at least six resisting members. Often, in order to resist the force of gravity better, there may be seven members. Each of the members contains a load cell to obtain force data from the motor. Usually, to prevent the precision load cell from being subjected to moments, each cell is protected on each end by universal flexure joints which can only transmit axial forces through the load cell.

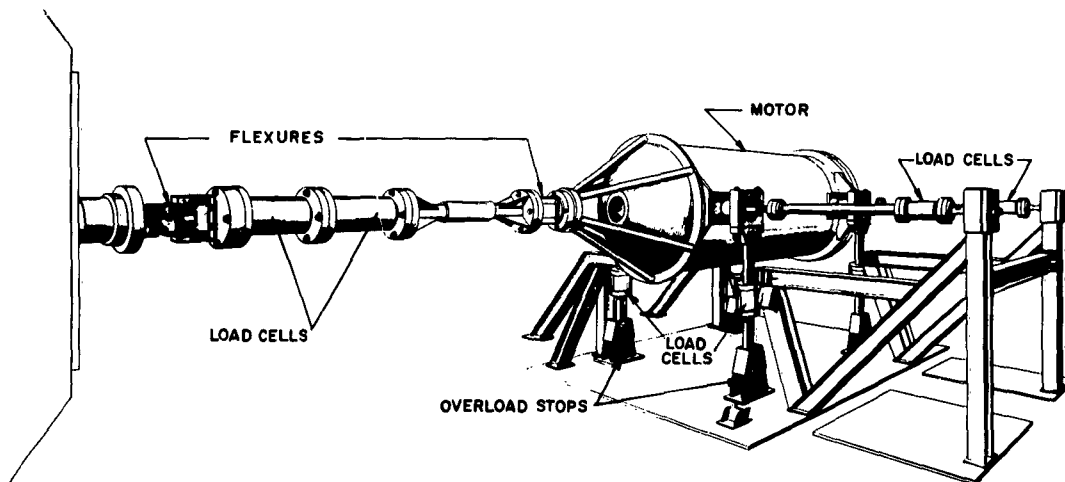
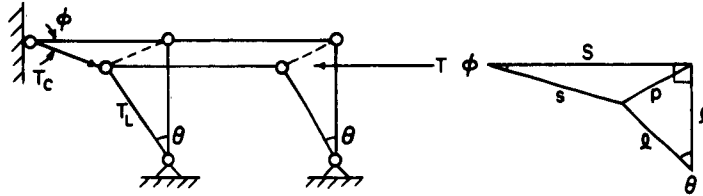


FIG. 3. Six-Component Thrust Stand Configuration.

Theoretically, this combination of six or seven force-sensing elements and known member alignments can determine the complete static thrust output of a solid-propellant rocket. In short, the known load-cell outputs and initial member alignments form a system of six to seven vectors, the sum of whose components is equivalent to the rocket-motor thrust. However, empirical experience often departs from theoretical conclusions. The linkage, which is composed of six to seven bars, is flexible since only by permitting deflections in the load cells of the system can the force be measured. Also the flexure joints (in order to isolate the load cells from moments) are composed of thin leaf flexures working at a high-stress level. All this adds up to a relatively soft linkage system. This soft system, which has usually not been precisely aligned initially, will deflect further under load. And, if the spring constants of the various linkages are not known, the stand will be distorted into a configuration that can cause relatively large errors. (Known errors of 2% have occurred in the authors' experience.)



In actual practice, however, this simple standard model cannot be used. The flexibilities of all six or seven members must be taken into account and an analysis will yield greater an-

deliberately getting involved in bending or shearing load cells. Therefore, the spring constant of the two universal flexures is usually as low as the load cell spring constant. An analysis of the flexure problem and formulas for design and evaluation are given in Appendix D. A further ramification of the foregoing discussion is the fact that the flexure-load cell member is flimsy in the sense that it cannot take high overloads. This leads to the overload harness concept which will be discussed later.

INITIAL STAND ALIGNMENT

The requirement for measuring thrust vector control (TVC) leads to the necessity for accurate side support member alignment. Lengthening these side support members decreases the relative angular alignment required. A sample calculation on this problem is given in Appendix B. With the assumed configuration and loads, in all force readings the lateral members must be aligned within $0^{\circ}-05'$ and the motor and thrust train must be aligned within $0^{\circ}-00'-21''$ to maintain 0.1% accuracy.

This calculation demonstrates the advisability of accurate initial stand alignment. If the requirement for accurate and quickly obtained initial stand alignment is made one of the primary specifications early in the thrust-stand design, the problem can be solved with less difficulty. To attain a facility accuracy of 0.1%, the alignment equipment will almost certainly involve the use of optical tooling. A planned program for stand alignment starting at an early stage in stand design will yield dividends later in terms of shorter stand alignment times as well as in increased accuracy. Here again the thrust bay will influence the relative ease with which the optical tooling and its special requirements are incorporated. Usually the system of base lines and sighting points will be external to the thrust stand proper. A relatively uncluttered bay will assist in this requirement. Figure 5 illustrates a possible optical alignment layout.

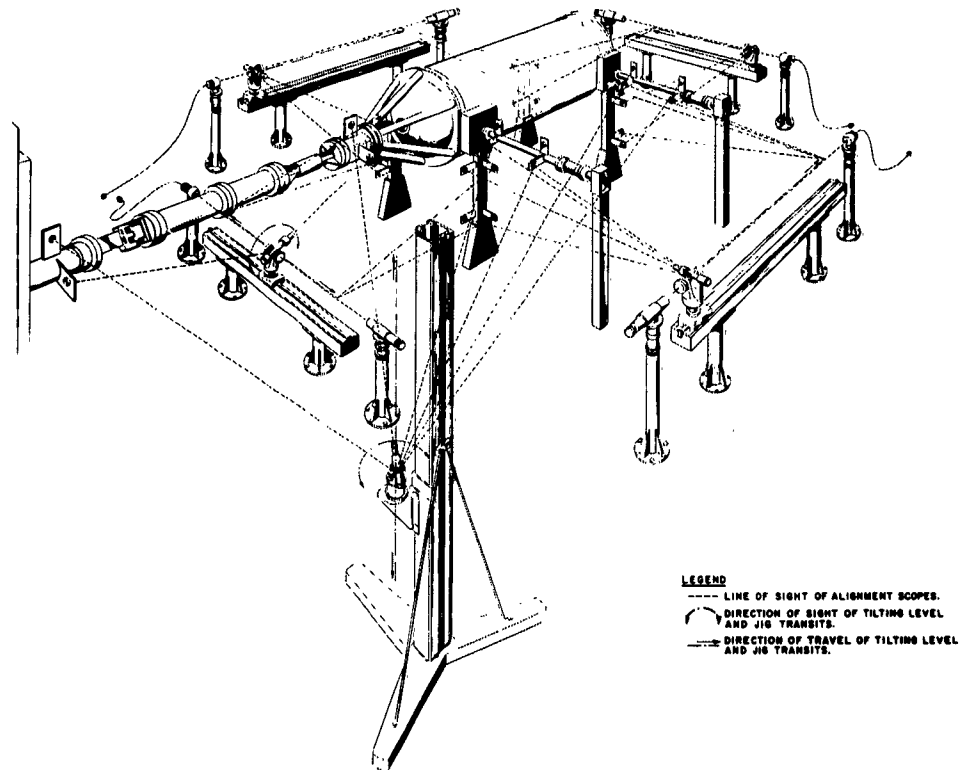


FIG. 5. Stand Alignment Instrumentation Array.

EASE OF ASSEMBLY AND DISASSEMBLY

As the size of the stand increases, the problem of fastening the components together becomes more difficult, especially when the goal is to maintain linear spring constants in both tension and compression. With stands of large size, threaded joints are impractical in the main thrust assembly if ease of assembly and stand linearity are desired. The best example of the handling problems created by large threaded joints is apparent in the piping industry where experience has dictated that piping in sizes over 2 or 3 inches is best joined by flanged fittings rather than threaded joints. Hence the use of flanged joints between stand members is one solution to the fastening problem, to improve the linearity and assist in solving the frequency-response problem. Flanged joints must, however, be designed properly to yield reasonably linear spring constants.

It is evident that a normal flanged joint (Fig. 6) will have a softer spring constant in tension than in compression due to the difference in the cross sectional area of the flange bolts taking the tension load and the flange faces taking the compression load. One solution is to recess the mating faces of the flanges so that they are in contact only at the outer edges. Thus, under tension and compression, the flanges will 'diaphragm' somewhat equally in both directions. The fastening bolts must be torqued to a preload value that will prevent the joint from separating under tension loads. A comparison of the data in Fig. 6 with that in Fig. 7, in which these design principles were used to build a flange-mounted 100,000-lb load cell, show that nearly equal diaphragming can be accomplished very well with this type of flanged joint. Figure 7 also shows the difference in the tension spring constant when the flange bolts are not torqued to sufficiently high values.

As the designer proceeds he should keep the assembly problem in mind at all times because it is easy to build a part that is not easily put in place or in which the fastening bolts are difficult or impossible to get at with standard tools. Some common design mistakes often made include not providing a wrench flat or other holding point on a rod member, lack of adjustment clearance for stand alignment or normal motor dimension tolerances, or the use of several sizes of fasteners in one assembly, requiring a large number of tools to be at hand. Also, the assembly sequence should be kept in mind during design to preclude creating unsafe working conditions and to insure that conflicting assembly steps do not make assembly difficult or impossible.

If screw-jack adjustment fittings are used in the stand members to permit alignment, they need to be designed so that there is no looseness in the thread fit to cause 'shake' and consequent instrumentation noise and stand nonlinearity. Due to the difficulty of making a zero tolerance thread it is preferable to lock the threaded joint to guarantee a zero shake condition.

MODULAR CONCEPT

The modular concept of stand design becomes almost a necessity in accurate six-component stands since the stand is composed of six or seven long members that must be taken apart for access to the load cells. This modular concept makes it possible to reduce the weight of individual members so that they may be handled more easily and also permit more flexibility in providing for future changes in the size of the motors to be fired with a minimum of hardware modifications. The use of the flanged module, combined with the ability to support the motor in the damage-control harness, can permit removal of load cells for prefiring calibration even after stand alignment.

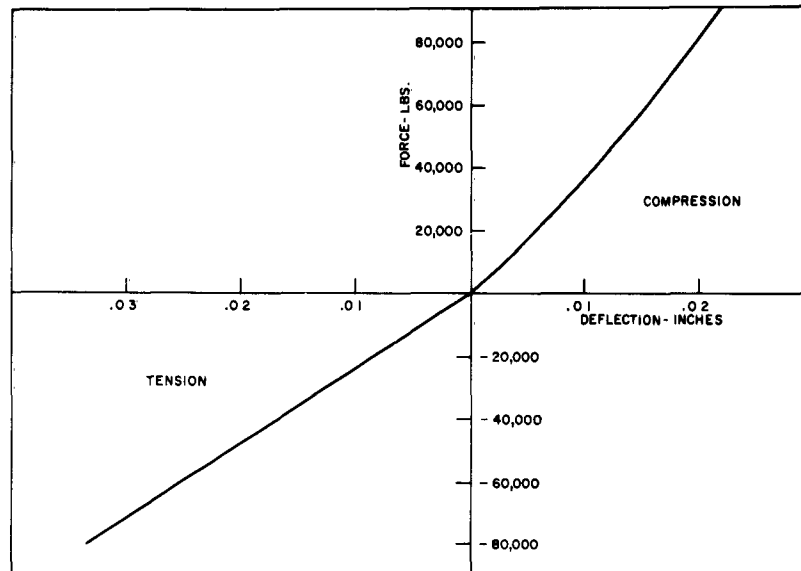


FIG. 6. Typical Flanged Joint Load-Deflection Curve.

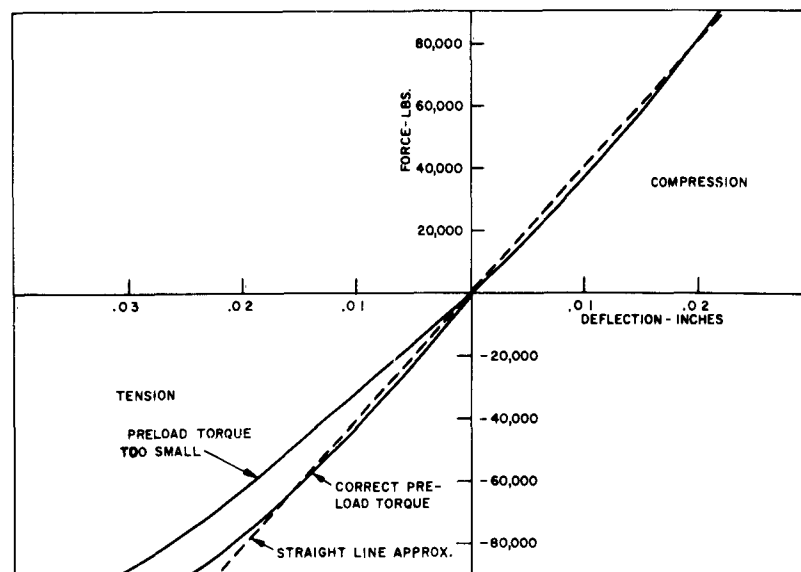


FIG. 7. Improved Linear Joint Load-Deflection Curve.

Another advantage that has recently come to light is that of lower replacement costs due to damage caused by motor malfunctions. This feature is illustrated by the analogy to an automobile which has replaceable fenders, doors, etc., so that only the damaged parts will need to be replaced after an accident. Recently at NOTS two nearly identical motor blow-ups on two differently constructed stands showed the value of the modular stand construction. The stand that was built of one large welded framework of plates and beams was a total loss although only a few plates were warped or bent, while the modular stand suffered only about a 30% loss and (with available spare parts on hand) it was put back in operation within a very short time.

DAMAGE CONTROL

The extreme lateral flexibility of the support and load measurement members needed to produce a 0.1% stand makes the danger of a catastrophic collapse due to sudden overloads from motor malfunctions or excessive misalignment a major consideration. Since efficient flexure design requires that the working-stress levels be relatively high for good flexibility, the margin of safety for failure is generally not much greater than two or three times the working stress. Past thrust-stand motor malfunction experience has shown that loads on the order of ten times the normal force can be produced (the loss of the complete aft motor closure, for example) yet the motor must be contained by the stand if possible. The most obvious method to contain these large forces is to build a restraining structure around (but not touching) the primary stand to pick up excessive deflections from overloading.

In order to prevent damage to load cells and flexures, overload or shear pin slip joints can be used successfully. One bad malfunction in which the load cells and flexures are saved will more than pay for the overload harness. A shear pin can be readily changed to allow any 'risk factor' that may be desired with a particular motor. Experimental data on steel shear pins of large size (capable of withstanding a 100,000-lb load) show excellent predictability and repeatability on shear stress failure values. The authors were able to predict within 5% the static failure loads of a 'V' notched shear pin made of 4130 steel with varying depth of notch.

It must be remembered that the loads encountered by the damage-control structure are dynamic loads and the forces produced by restraining a moving mass of large size are often (due to momentum) several times larger than the thrust or force producing the movement. For this reason the flexibility of the structure should be taken into account. The following equation relates the restraining force, F , the weight of the moving parts, W , the thrust or motivating force, T , the velocity, V , attained by the weight at impact, and the deflection of the restraining structure, δ :

$$\frac{F\delta}{2} = \frac{WV^2}{2g} + T\delta$$

Thus, the energy absorbed by the structure is equal to the kinetic energy of the moving weight plus the work done by T. F is then the maximum force that will occur and will be the design load for an expected overload.

The damage-control structure can be used for other purposes, also. It can be used to support the stand members during assembly and alignment, to apply loads on the primary stand for evaluation work, to support work platforms for maintenance and assembly and possibly to serve as a reference framework for alignment. In addition, it can be used to support the motor after assembly and stand alignment so that load cells can be removed for prefiring or postfiring calibration.

EASE OF LOAD CELL CALIBRATION

There are two schools of thought concerning load-cell calibration: in-place calibration and individual calibration of removed load cells. At first glance the in-place method appears to be the best operationally but from the standpoint of stand design and accuracy it poses some problems.

As discussed previously, the flange-jointed modular concept and the damage-control harness lend themselves to easy removal of load cells without building additional expensive calibration equipment or disturbing the alignment of the stand. Assuming that the stand is properly designed so that errors due to stand deflection and restraint are sufficiently small, the cells can be calibrated before and after tests under controlled conditions to yield as high an accuracy as the equipment and laboratory setup allow. The in-place method is more desirable, however, from the standpoint of time and labor involved in calibration, although it requires additional structure, either in the damage-control harness or external to the stand, through which the calibration loads are applied. These loads will involve both tension and compression forces for lateral load cells, so the equipment must be designed so that loads can be applied in both directions.

There is some question as to how an in-place calibration of a large thrust stand should be accomplished and how this information can be used to assess the test data. A discussion of the state-of-the-art in calibration sheds some light on the picture. The National Bureau of Standards is capable of performing calibrations accurate to 0.01% by using dead-weight equipment for loads of up to 111,000 lb. Loads above this figure can be certified by using single or multiple gages calibrated by

dead-weight equipment. Most of the large load-testing machines for materials testing are calibrated to 0.5%. In order to keep from sending load cells to the Bureau of Standards for each calibration, proving rings are generally used which have been calibrated by dead-weight testing or by comparison with another proving ring tested by dead-weight equipment. It appears that, for each step removed from dead-weight equipment calibration accurate to 0.01%, accuracy is lost by a factor of 10. So unless one builds a dead-weight calibration setup similar to the NBS equipment, the stand builder is forced to use a proving ring (which can be no more accurate than 0.01%) as a standard in order to calibrate the load cells to 0.1% at best. This is assuming ideal (laboratory) conditions during and after calibration which is hard to guarantee in the field particularly when the cells are installed in the stand and subject to overall temperature and stand-deflection effects. As an example, for each degree Fahrenheit temperature change from the calibration temperature, a Morehouse proving ring with a certified accuracy of 0.1% is subject to a change in calibration of about 0.015%. This means that the temperature during cell calibration and thereafter must not vary by more than 7°F to maintain 0.1% accuracy and if the proving ring is only 0.1% to start with, any temperature variation will reduce the accuracy to less than that desired.

Immediately then it appears that even under the best of field conditions, in-place calibration of a large test stand to an accuracy of 0.1% is extremely difficult if not impossible in the present state-of-the-art. Removal of the load cells before and after tests would at least allow laboratory conditions to prevail during calibration.

Another big question is how to perform the in-place calibration. Theoretically, the best way would be to apply a known force vector to the stand and measure the resulting forces at all load cells. Assuming this could be accomplished, occasionally the load cells would still need to be calibrated individually (either in place or removed) to guarantee continued accuracy and repeatability. However, in stands of large size, the stand may deflect in any direction by as much as 1/4 inch or more. Unless long flexured columns are used to apply these loads, appreciable error may result from off-axis alignment or friction restraint as previously cited in regard to the length of the stand restraining members. Also, if calibration of the lateral load cells is not conducted at the same time the stand is being subjected to the expected main thrust loading, appreciable errors can occur due to the natural lateral thrust-force component generated by the stand's lateral deflections. The expected motor expansion of 0.5 inch or more can grossly misalign the rear stand members and cause main thrust errors that may be overlooked when normal calibration techniques are used. This expansion also changes the point of application of the TVC force in relation to the force measuring members. Simple calculation of typical stand configurations indicates that these errors may be in the order of 0.5% or more depending on the precision of initial alignment.

The above considerations point up the fact that in reality the in-place calibration scheme may not be as easy and useful as it appears to be. A more satisfactory procedure might be to use a combination of the two methods in which each cell is removed and calibrated individually but the stand as a whole is calibrated by applying known force vectors to it by accurately measurable means. This could be done by using a long flexured column through which any combination of thrust and side-force vector could be applied to most closely simulate the dynamic condition for the stand. To do this, a movable buttress would be required and a column sufficiently long to allow angular misalignment with the stand main axis of about 6° (lateral force 10% of main thrust). Provision must also be made for a very precise angular measurement with respect to the stand reference lines. The problem of motor expansion, which probably causes the largest single deflection in the system, might be taken care of in one of several ways; i.e., by using separate flexures at the rear motor attachment to allow motor growth without misaligning the rear members, by intentional misalignment of the rear members so that they come into alignment during firing, or by monitoring the movement of the rear members and correcting the data analytically. The data from these tests could then be programmed for a computer to reduce data from stand load cells to acquire thrust vector data.

One technique that has been used to evaluate the dynamic response of a stand is known as 'twanging'. This consists of loading the stand and suddenly releasing it by using explosive bolts or some other method. The load-cell traces can then be examined for stand natural frequency, linearity of the stand members, damping, structural resonances, sloppy joints, etc. Examples of the information that can be obtained from this twanging data are shown in Figs. 8 and 9. Figure 8 is the load-cell trace from an inexpensive, single-component stand after release from a 50,000-lb tension load. The difference in spring constant for tension and compression is obvious from the nonsymmetrical wave form. It would be difficult to determine the true thrust under dynamic conditions with this type of nonlinearity. Figure 9 is the load-cell trace from a more sophisticated 3-component stand in which more effort was made to make the spring constant linear. The improvement in spring-constant linearity is apparent. The approximate spring-constant curves shown in these figures were determined experimentally for the tension side during the test and by simulation on an analog computer for the compression side. The shape of the spring constant curve in compression was varied until the computer duplicated the response curve from the stand. This twanging procedure is also useful in instrumentation prefiring checkout.

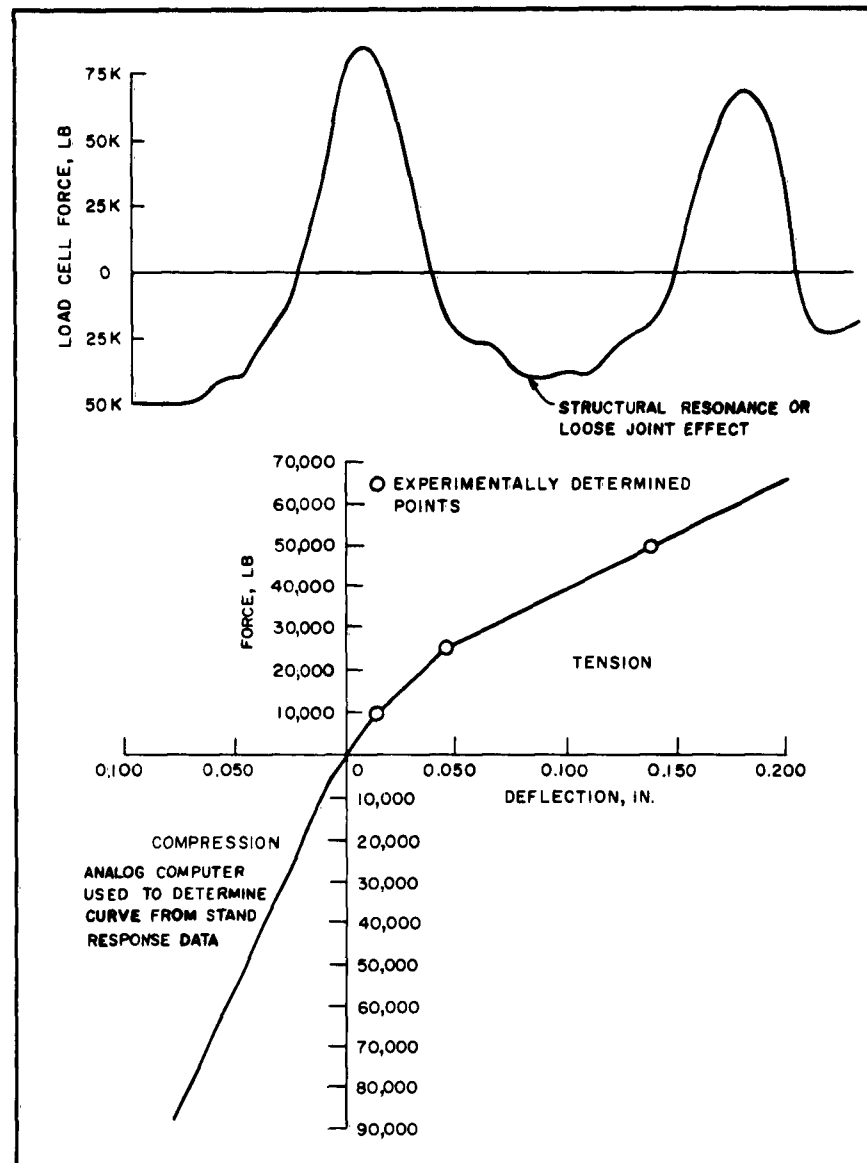


FIG. 8. Load-Cell Trace From Single Component Stand With Nonlinear Spring Curve.

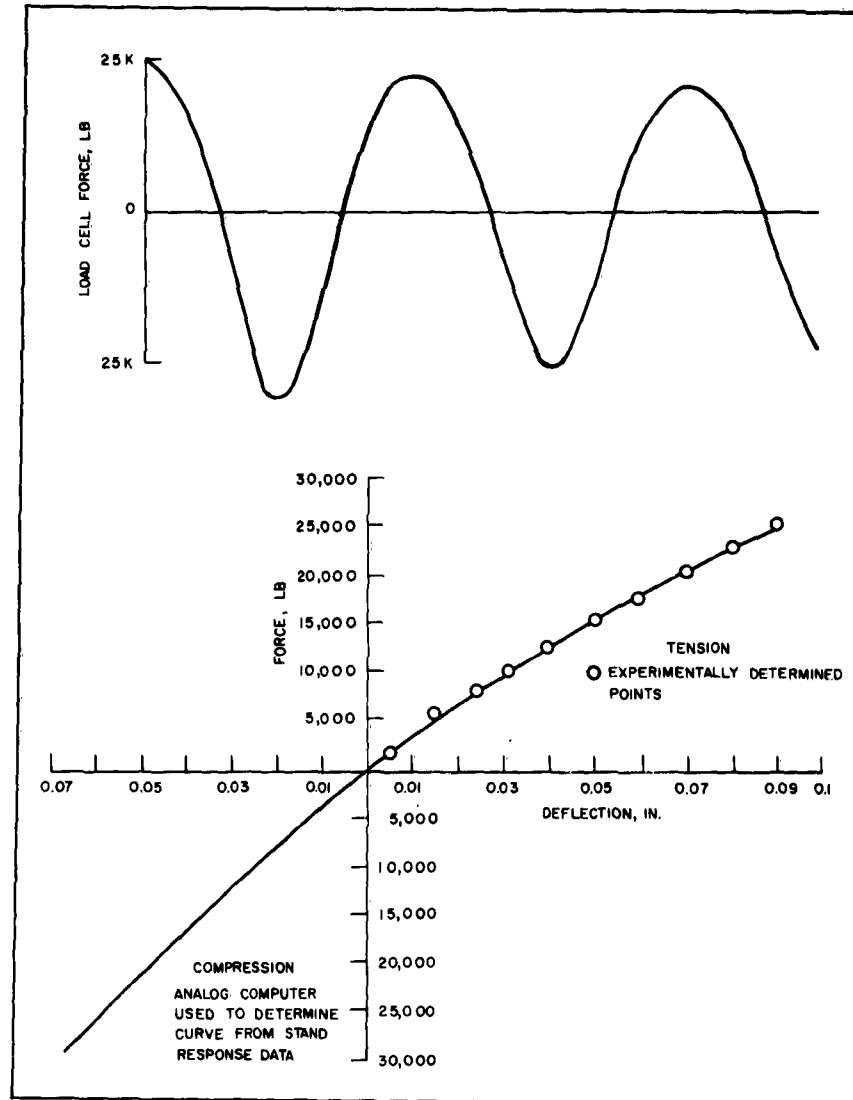


FIG. 9. Load-Cell Trace From Three-Component Stand With Improved Spring Curve.

ENVIRONMENTAL CONTROL

The present trend in static testing of large rocket motors is to simulate as closely as possible the physical environment which will surround the motor during actual flight. The present state-of-the-art permits only a few of the actual conditions to be approximated; i.e., motor restraint, firing attitude and case stressing, temperature, pressure (altitude), and possibly vibration to some extent. The question then arises as to whether to sacrifice accuracy for closer simulation; it sometimes becomes very difficult to get both. Perhaps the answer lies in the basic requirements for a specific facility or a particular firing. It may be possible with clever design to build the stand so that any degree of accuracy and/or simulation can be achieved to meet the particular test requirements without unduly sacrificing the other parameters for other tests.

The first of these parameters, motor restraint, is becoming a more important factor in test simulation as motor designers are able to increase the motor diameter and reduce the chamber-wall thickness. Calculations indicate that a large fiberglass-case motor may expand in diameter by 1/2 inch or more and in length by well over an inch. Any enclosing harness or stand structure which resists this expansion may both adversely influence stand accuracy and the evaluation of the motor design by degrading the accuracy of the simulated flight conditions. This relatively large movement due to expansion further strengthens the earlier conclusions about using long-flexured stand members to reduce the restraint forces and the resulting errors due to stand movement.

Similar to this is the question concerning firing attitude. In general, a horizontal stand is easier to design, less expensive to build, and presents fewer operational difficulties than a vertical stand but flight conditions cannot be simulated as well as they can be with a vertical stand. In the large motors now being built simulated flight parameters are increasing in importance and the firing attitude may significantly alter motor performance. Therefore, it is necessary to understand the problems associated with vertical six-component stands and to try to find solutions that will assure building ease and operational qualities equal to those of the horizontal stand. The method of attaching the motor to the stand is also of prime importance. The motor should be mounted so that the loads in the motor case due to the motor's own weight and thrust are applied as nearly as possible as they will be in flight. It is more difficult to incorporate the jetavator or side loads into the case as they occur in flight since, normally, these forces will be taken out near the nozzles by the lateral restraining stand members during a static test, whereas in actual flight they cause a bending moment force to be applied to the motor case. This is one condition which may have to be compromised in order to measure the overall forces in a direct manner.

Temperature control is necessary in all large thrust stands because (1) rocket propellants are sensitive to temperature changes as far as performance is concerned and may produce very undesirable characteristics under large temperature changes (generally, normal room-temperature variations of 5 to 10 degrees is adequate control) and (2) load cells are temperature sensitive. Also the expansion and contraction of large stand parts under temperature changes may affect alignment, especially if the stand is exposed to sunlight for any length of time. Painting parts white greatly helps to reduce sun-heating effects. The use of portable buildings is effective in controlling prefiring temperatures and may be adequate for the motor itself since most large motors can be exposed to out-of-limit temperatures for short periods without trouble. However, temperature-variation effects on the stand parts and load cells should not be ignored. Shielding, insulation, or controlled-temperature blankets might be used to protect critical stand parts.

High altitude simulation on a static-fired rocket motor is one of the more recent large thrust-stand capability requirements. Simulation of the reduced outside pressure experienced at altitudes of 50,000 to 100,000 feet has been successfully accomplished with large size motors. This requirement presents many problems to the stand designer not the least of which is the high cost of building a vacuum chamber large enough to contain an accurate six-component stand. However, it may be necessary to simulate the altitude at the nozzle end of the motor only. In this case, the relatively small vacuum chamber needed can be attached to the nozzle end of the motor by a flexible bellows that will produce negligible interference with the stand movement.

A water-cooled diffuser tube attached to the vacuum chamber through which the exhaust gases escape is the usual method of maintaining the initial low pressure in the semi-evacuated chamber. The action is similar to that of a steam ejector with the low pressure suction vent closed off to maintain low pressure at the rocket nozzles. Both single-wall, spray-cooled, and double-wall water-jacketed diffuser tubes have been used successfully.

If data requirements make it necessary to subject the entire motor to the simulated altitude environment, the 'canned' motor concept should be investigated. By using flexures (to permit expansion) the motor could be installed in a close fitting can with a vacuum capability attached to the diffuser tube by a flexible coupling. The stand force-measuring members would then attach to the can instead of the motor as in conventional stand design. The can could be used to provide the temperature conditioning environment and, in addition, it might facilitate motor-loading and reduce preparation time.

MASS MEASUREMENT

Continuous mass measurement of a rocket motor during burning, which has long been desirable from the standpoint of thrust stand users, has remained an unsolved problem in stand design. The advantages of measuring mass or weight continuously during burning are obvious, especially if a motor fails at some point before burnout, thus rendering useless the present technique of calculating mass by using the end points of mass and pressure-thrust information. Continuous mass measurement permits motor-development people to determine instantaneous specific impulse and also assures more accurate assessment of thrust data, especially in vertical stands. The use of continuous-mass information may also be used to isolate thrust-stand 'ringing' from the thrust data for more accurate measurement during transient conditions. This technique of data combination (described in NAVWEPS Report 7569, Ref. 3) is more easily accomplished if the stand designer has been careful to provide the linear spring constants in stand members as described earlier in this report. Figure 10 shows how this can be used to yield true thrust data during sharp transients by removing the $M\ddot{x}$ transient factor which is due to stand ringing. This requires good mass information, preferably better than the 5% data accuracy obtained using present techniques.

The most obvious drawback to measuring mass continuously by weighing with load cells is that, if the thrust vector varies from the true 90° to the axis of the weighing load cells, an error due to the component of thrust in that direction will be introduced. If the lateral-thrust information is not better than 5% then the mass-measurement accuracy will be no higher than this. When jetavators or other control systems are involved this too increases the weighing problem.

A new technique which has been partially tested and shown to be promising is that of exciting and measuring the natural frequency of the stand as a function of overall stand-rocket-motor mass. This technique and the results of the first tests are described in NAVWEPS Report 8354, Ref. 4. The early theory and a discussion of how this technique might be used appear in NAVWEPS Report 7741, Ref. 5. This technique involves the use of a motor-stand assembly mounted on springs which allow the assembly to vibrate in a translation mode perpendicular to the main thrust axis, thus decreasing its influence on the thrust data. The spring-mass system is vibrated at its natural frequency (less than 1 g) by a variable-speed motor-mechanical shaker. A measurement of the change in natural frequency can then be related to mass change as shown in Fig. 11.

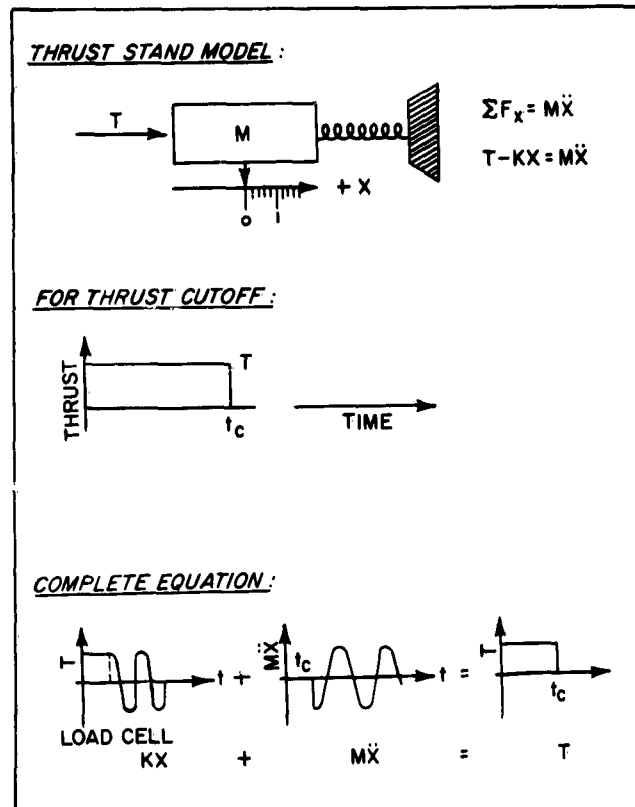
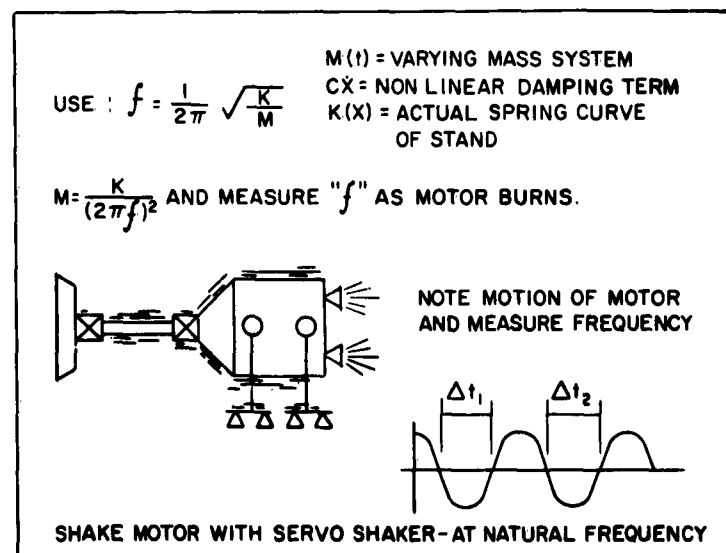


FIG. 10. Data Combination Correction Procedure.

FIG. 11. Calculation for Mass Measurement Showing Schematic of Motor With Servo Shaker at Natural Frequency.



A servo-control system, which controls the shaker-driving motor to drive the system at its natural frequency, makes use of that property of a vibrating system which causes the motion of the mass to lag the driving force by 90° at resonance. The servo then controls the speed of the shaker-driving motor so that this 90° relationship is maintained and the system is 'locked' onto the natural frequency. A schematic of the system is shown in Fig. 12.

The design of a stand for use with this type of system requires careful planning to avoid compromising the primary data-gathering system. Certainly, in this application, long stand members to accommodate the motion due to stand vibration at low frequencies without excessive restraint and malalignment are even more of a necessity. Other problem areas encountered in the first tests include: (1) difficulty in obtaining accurate measurement of the spring constant of the stand, (2) unequal damping from front to rear on the spring system, (3) c.g. shift during burning, (4) structural resonance of stand members, and (5) degrading effects of vibration modes other than translation. These problems and their suggested solutions are discussed in more detail below.

1. The spring constant of the spring-mass system must be known in order to solve the equation for mass. This spring constant is composed not only of the springs themselves, but also of the complete supporting stand members (including load cells and flexures), and joints. An in-place experimental determination seems to be the best way to determine the spring constant. Again, care should be exercised in making the entire spring constant as linear as possible.

2. Unequal damping of front and rear spring-mass systems will cause unequal amplitudes and introduce errors into the control system. The structural damping of the axial thrust assembly generally results in more damping at the forward end. Experience has shown that this may cause a 200-300% unequal amplitude from front to rear. Displacement

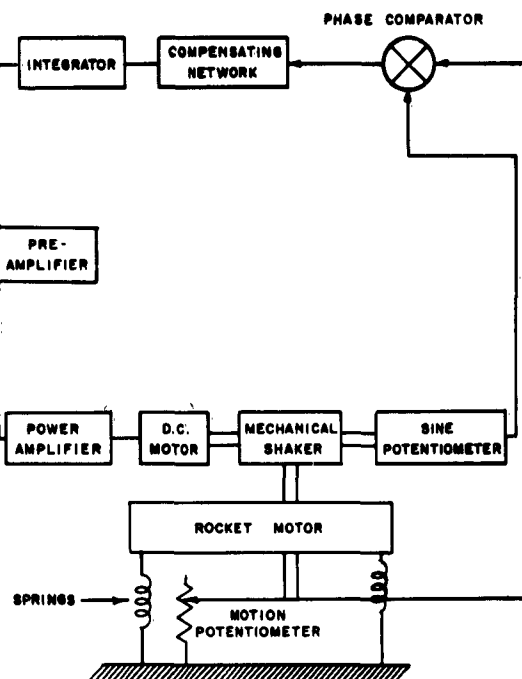


FIG. 12. Schematic Diagram of Mass Measuring System.

versus frequency is plotted for a loaded motor in Fig. 13 and for a burnt motor in Fig. 14. The relative displacement fore and aft also varies as the mass of the propellant changes (the rubbery propellant mass can add damping) so that controlling the amplitudes by means of individual dashpots fore and aft may require continuous adjustment of damping. A torsional damper, which is attached to front and rear spring systems and comes into action only if unequal amplitudes are present, appears to be a more efficient scheme since minimum damping is desirable for good frequency response.

3. The shift in center of gravity during burning can cause the stand to become coupled so that the shaking force no longer acts through the c.g. It was found, however, that with the stand used for these tests the c.g. shift was less than two inches; with springs and shaker set for average c.g. no apparent difficulty due to this factor was experienced. Analog computer simulations of the system verified that c.g. shifts of as much as six inches can be tolerated for this particular configuration.

4. Structural resonance in stand members may cause trouble if the frequency falls within the range of frequencies traversed during firing. This is especially true when the members have large masses (load cells, etc.) associated with them. These resonances will show up as spikes in the plot of amplitude versus frequency and their size, relative to the main translation-mode amplitude, denotes the degree to which they are negligible or must be remedied. The axial-thrust assembly, because of its long length, large mass of load cells, flexures, etc., is probably the most likely to offend. Relocation of components or the use of stiffer members in bending will help raise these resonances out of operating range. The mountings which fasten the shaker to the stand must also be designed to contribute no restraint on the stand movement; yet, to maintain the 90° relationship, they must be stiff enough in the direction of shaking force to transmit the motion to the mass-spring system without phase shift. For example, the natural frequency that the mounting system must have for a spring-mass system with 1% of critical damping and a natural frequency of 15 cps can be calculated for any allowable phase shift by:

$$\tan \phi = \frac{2 \zeta \frac{\omega}{\omega_n}}{1 - \left(\frac{\omega}{\omega_n}\right)^2}$$

ϕ is phase angle between shaker force output and force input to the stand

ζ is the damping factor, C/C_c

ω is the natural frequency of the stand (assumed as 15 cps)

ω_n is the natural frequency of the shaker mounting system

FIG. 13. Rocket Motor and Stand Displacement as a Function of Frequency (Live Rocket Motor).

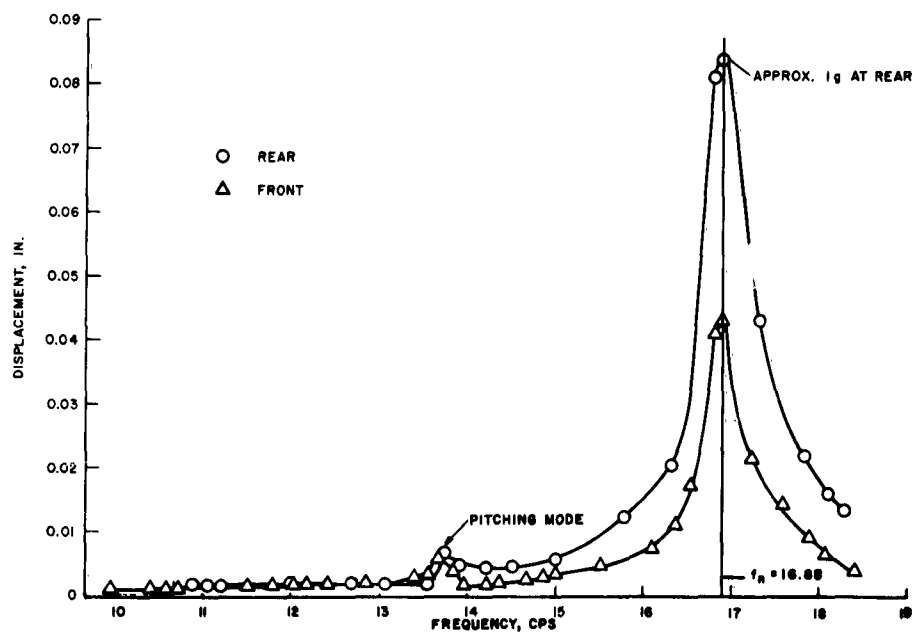
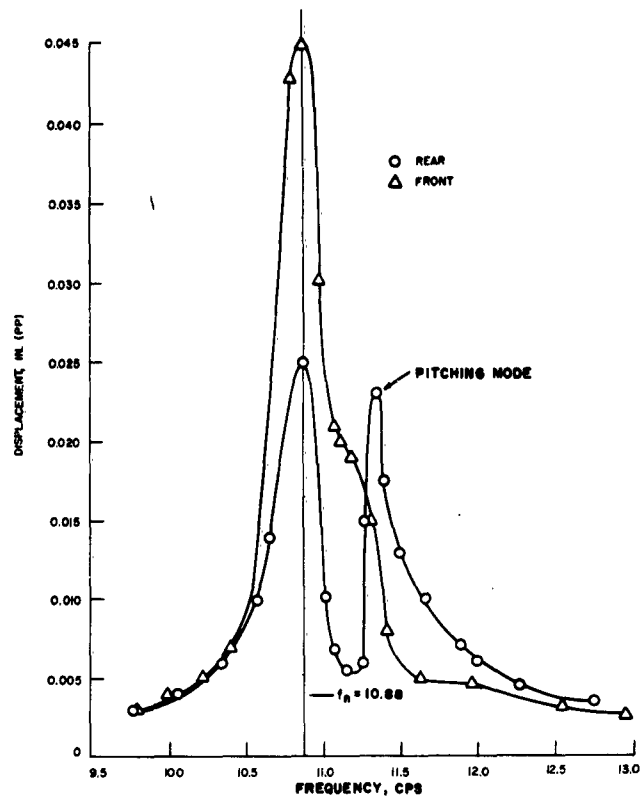


FIG. 14. Rocket Motor and Stand Displacement as a Function of Frequency (Burnt Rocket Motor).

If the maximum allowable phase-angle shift between the force output from the shaker to input into the stand is 0.5 deg, $\frac{\omega}{\omega_n}$ is computed to be 0.266, and the shaker and its mounting natural frequency must be at least 56.5 cps.

5. The most undesirable effect encountered in system tests was the appearance of the pitching mode at a frequency close to that of the translation mode. Since the 90° phase relationship between force and displacement applies to this mode also, the control servo can lock onto this spurious mode or be sufficiently confused by its presence to seriously degrade performance. It can be seen in Fig. 14 that the pitching mode (13.7 cps) occurs at a lower frequency than the translational mode (16.88 cps) with the burned motor but with the unburned motor, shown in Fig. 13, the pitching mode (11.3 cps) is above the translation mode (10.88 cps). This means that during burning the two modes will cross over and cause confusion in the control system as they begin to separate.

Two approaches can be made to eliminate undesirable modes in an existing stand: (1) damp them out or (2) raise their frequency out of the operating range. To accomplish this, a torsional damper or spring can be used without interfering with the other mode. It is much more desirable, however, to anticipate this problem during the design stage and design a stand having natural frequencies outside the pitching mode frequencies, rather than having to adjust finished hardware in the field.

The results of the first live-firing test proved that the spring-mass servo control method of obtaining continuous-mass information is feasible. Even with the breadboard prototype system, mass information within a 2% agreement of the accepted standard method of computing mass was obtained during most of the firing time. At about ten seconds after ignition, the pitching-mode frequency crossed the vertical translation-mode frequency and seriously interfered with the control servo. Test results are plotted as mass versus time in Fig. 15. More than 50% of the data is within ±2% of the calculated values and during only about 15 sec of the approximately 60-sec burn time is the data worse than 5% due to the pitching-mode interference. Analog computer studies of the test data were conducted to facilitate a closer investigation of overall system response and to study the effects of various system changes. One interesting result was that, during the analog study, a mechanical-coupling term had to be added to the equations of motion to duplicate the test data. (This was found to have resulted from the structural resonance of the axial-thrust assembly which had a natural frequency very close to the translation mode at burn-out.) Another fact that emerged was that some of the jetavator or lateral-force programs imposed on the operating system seemed to improve the operation of the control system by smoothing out the 'hunting' oscillations of the servo. Care does need to be taken, however, to insure that these lateral-force programs are neither cycling near the stand natural frequency nor in the same plane as the shaking force or the vibration amplitude may exceed the limits set for safe operation of the system.

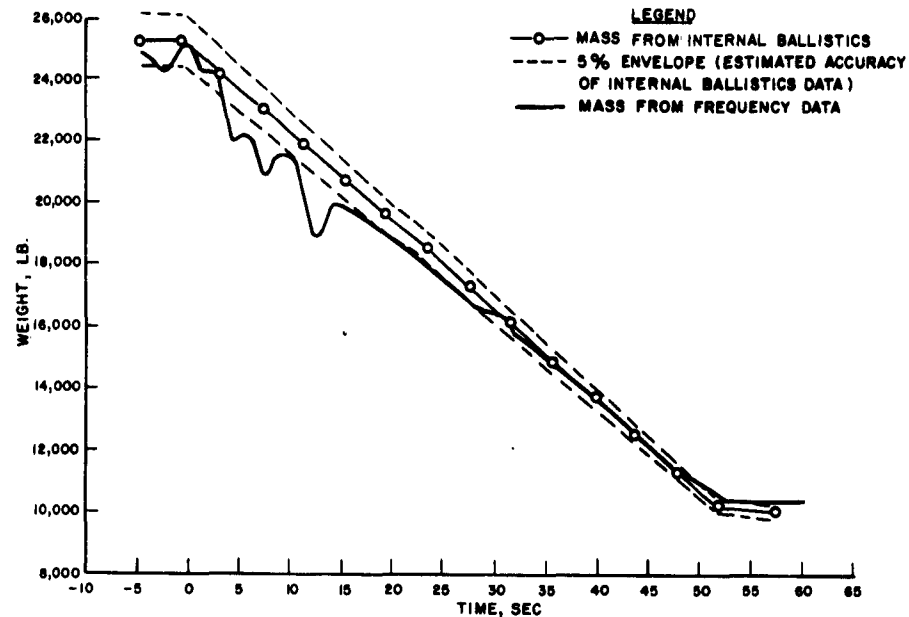


FIG. 15. Vibrating Mass as a Function of Burning Time.

THRUST STAND DESIGN PROCEDURE

1. Itemize Stand Requirements

- Number and type of measurements desired
- Accuracy
- Test conditions (attitude, environment, bay size and space limitations, etc.)
- Motor specifications and configuration (handling, attach points, temperature limits, etc.)
- Cost and time limitations

2. Preliminary layout of motor-stand configuration based on a, c, and d above.

3. Preliminary calculations to verify basic configuration and to establish approximate spring constants and lengths of members to provide the desired degree of accuracy.

Note: Simplified 2 or 3 degree-of-freedom equations are sufficient at this point. Spring constant limits will be governed by the load cells and the type of flexures to be used.

4. Choose flexure and load cell components based on preliminary calculations.
5. Draft preliminary design of stand members based on load cell and flexure choice and spring constants from paragraph 3 above.
6. Perform formal calculations on stand response and accuracy based on six degree-of-freedom equations and assumed forces acting on the stand. (A computer will be necessary for this operation assuming that these equations are already available.)
7. Complete design of stand members based on the principles outlined for optimum linearity, adaptability, convenience of assembly and operation, cost, damage control, etc., while maintaining the parameters obtained in paragraph 6.
8. Perform stand-evaluation program during and after fabrication and assembly of stand.
 - a. Perform static spring-constant measurements on stand members during fabrication and before assembly to check linearity and actual values. Modify as necessary.
 - b. Perform static spring-constant measurements on stand assembly to determine stand constants.
 - c. Perform twanging tests to obtain dynamic constants and stand response.
 - d. Refine paragraph 6 calculations using data from actual stand tests for accuracy studies and data reduction.

Appendix A

THRUST STAND GOALS

Quantity to be Measured:	FORCE - axial thrust and motor weight
Number of Such Measurements:	12
Accuracy Required:	$\pm 0.25\%$
Freq. Response Required:	50 cps. Transducer response to 1000 cps
Range of Variable:	Four transducers 0-10,000 lb for weight, eight 0-100,000 lb for axial thrust
Type of Detector:	
Amplifier Requirement:	
Total Cost per Channel:	
Purpose of Measurement:	Measure axial thrust and measure weight. For axial thrust, will use four transducers on high thrust tests, with a second set of 4 in tandem for accuracy check. The same transducers are to measure both forward and reverse thrust. For measuring weight, a set of four transducers will be located close to center of mass.
Factors Determining the Accuracy Requirement:	Accuracy requirements are established by the accuracy needed in impulse, specific impulse, and discharge rate. To be consistent with the reproducibility potential in propellant processing, a precision of 0.25% is sought. Absolute accuracy of the same degree will be useful when that pool of reproducibility in propellant quality is achieved.
Factors Determining the Frequency Response Requirement:	Frequency response is set primarily by the natural frequencies of the thrust stand-motor assembly. Consistency with specification on chamber pressure measurements is also desirable, is set by needs for

computing-desired quantities like specific impulse. A transducer frequency response of 1000 cps is desirable for interpretation of thrust transients due to nozzle blockage, leaks, charge failure (where starting time of the transient is most important and thrust stand frequencies do not dominate the determination).

Quantity to be Measured: FORCE - side components

Number of Such Measurements: 6

Accuracy Required: $\pm 2\%$

Freq. Response Required: 50 cps Transducer response to 1000 cps

Range of Variable: Initially, 0-10,000 lb

Type of Detector:

Amplifier Requirement:

Total Cost per Channel:

Purpose of Measurement: To measure forces off axis generated by jet deflection control, by jet malalignment and by weight components due to shift of c. g. from main weight transducer.

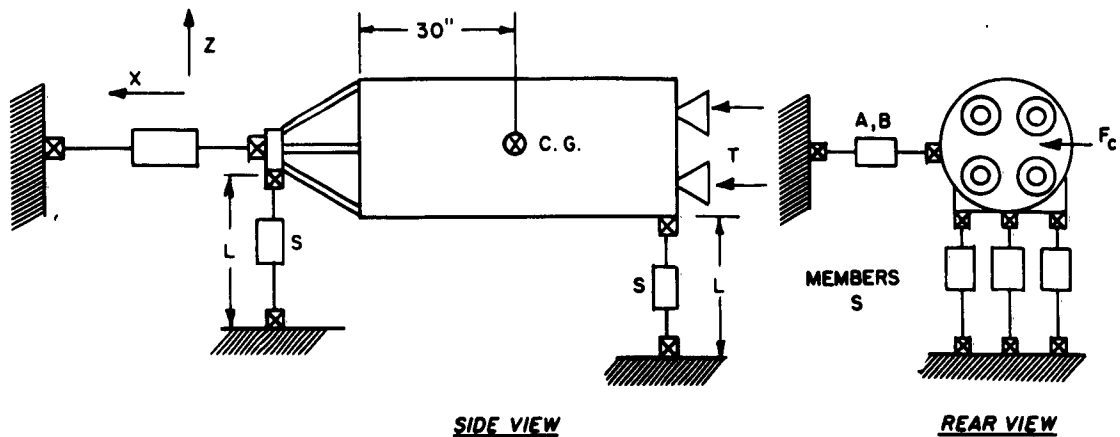
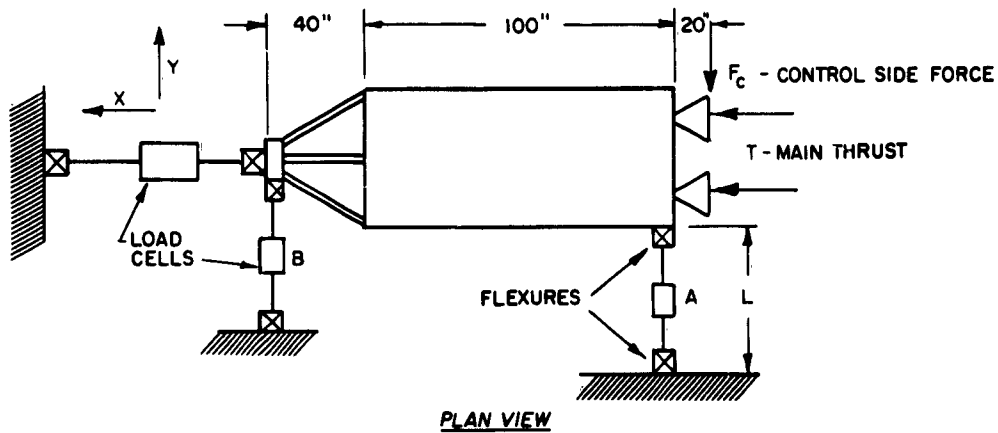
Factors Determining the Accuracy Requirement: Accuracy of forces due to jet deflection not of high level in a servo-controlled system-weight component will be only about 10% of total weight, hence required to only one-tenth the accuracy of the total weight.

Factors Determining the Frequency Response Requirements: Frequency response set by the duration of jet deflection of jet control cycles.

Appendix B

EXPLANATION OF NECESSITY FOR USING LONG STAND MEMBERS

Consider the following six-component thrust stand:



```

wt. = 25,000 lb
T   = 100,000 lb
fn = 20 cps (natural frequency in X direction)
Fc = 10,000 lb

```

A 20-cps stand will have a deflection under 100,000-lb thrust of 0.0977 inch. Adding 25% dynamic deflection due to stand ringing from thrust changes, the total deflection may be 0.122 inch. Let

$$\delta_x = 0.122 \text{ in.}$$

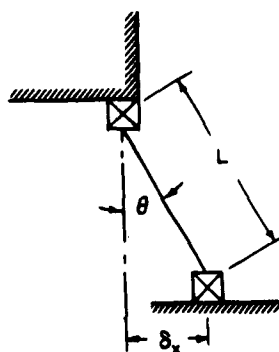
Lateral Members

The length of the lateral members, L , can now be calculated for any allowable error value in the main-thrust load cell.

For 0.1% accuracy in reading main thrust of 100,000 lb, the allowable error force must be less than 100 lb. Since there will be errors from other sources, consider 50 lb as the allowable error.

$$E = 50 \text{ lb}$$

As the stand deflects under the thrust load, the members assume an angle θ as shown:



From the stand geometry, the forces on the members A and B are:

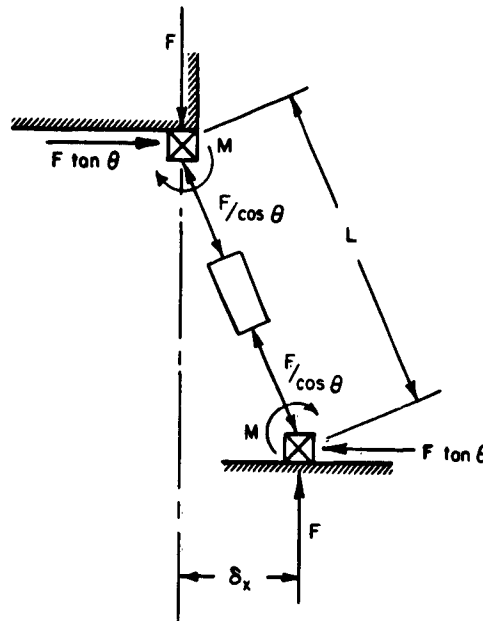
$$F_A = 11,420 \text{ lb (compression)}$$

$$F_B = 1,420 \text{ lb (tension)}$$

The forces on members S from the weight of the motor and stand are assumed as:

$$F_S = 8,333 \text{ lb (compression)}$$

The components of these forces then are:



The errors in the main-thrust load cell will be a combination of the following:

X components of the side forces and weight

Forces to bend the 10 flexures of the 5 members through an angle θ (moment M above).

(Although the malalignment stand error caused by the shortening of the side members will be ignored in this simple case, it should certainly be taken into account in designing a stand.)

For this example, a commercial universal flexure that represents a good compromise between high efficiency and low

cost is used. This 25K flexure costs \$440 and has an initial bending stiffness of 50.2 in-lb/deg. As flexures are loaded in compression or tension, their bending stiffness changes (by as much as 2 to 3 times their initial values) by a factor α . This 25K flexure under the various loads in this example has the following characteristics:

Member A: $K_A = 80.3$ in-lb/deg (each flexure)

Member B: $K_B = 30.2$ in-lb/deg (each flexure)

Member S: $K_S = 70.3$ in-lb/deg (each flexure)

Therefore, total K for the stand is:

$$K = 2K_A + 2K_B + 6K_S = 642.8 \text{ in-lb/deg}$$

The error due to this stiffness decreases the thrust reading by:

$$E_f = - \frac{K\theta(\text{deg})}{L\cos\theta} \text{ lb}$$

Letting $\sin\theta = \tan\theta = \theta$ and $\cos\theta = 1.0$ for small angles ($\theta < 1^\circ$):

$$E_f = - \frac{57.3K\theta(\text{rad})}{L} = - \frac{36,800\theta}{L}$$

and the errors due to the X components of the forces in the members are:

$$E_A = 11,420 \tan\theta = 11,420 \theta$$

$$E_B = 1,420 \tan\theta = 1,420 \theta$$

$$E_S = 25,000 \tan\theta = 25,000 \theta$$

So the total error is:

$$E = E_f + E_A + E_B + E_S$$

$$E = - \frac{36,800\theta}{L} + 11,420 \theta + 1,420 \theta + 25,000 \theta$$

and since $\theta = \tan^{-1} \frac{\delta_x}{L} = \frac{\delta_x}{L}$ and $\delta_x = 0.122$ in.

$$E = - \frac{4,490}{L^2} + \frac{4,270}{L}$$

Letting $E = 50$ lb, the equation becomes:

$$50 L^2 - 4,270 L + 4,490 = 0$$

and solving for L ,

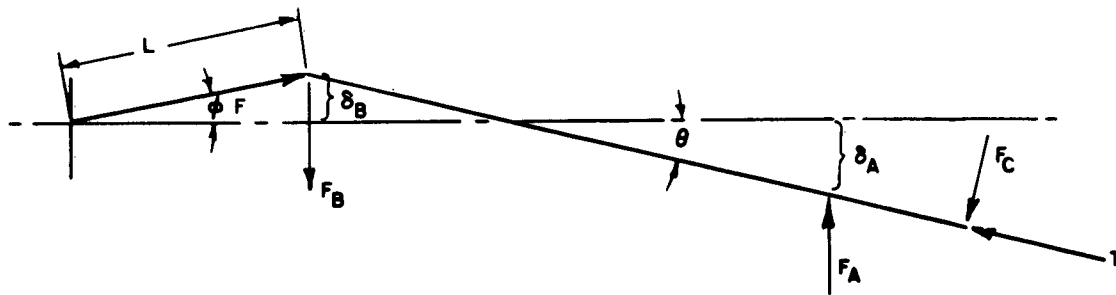
$$L = 84.3 \text{ in. or 7-ft long side members}$$

$$(\theta = 0^\circ - 05' \text{ angular displacement in side members})$$

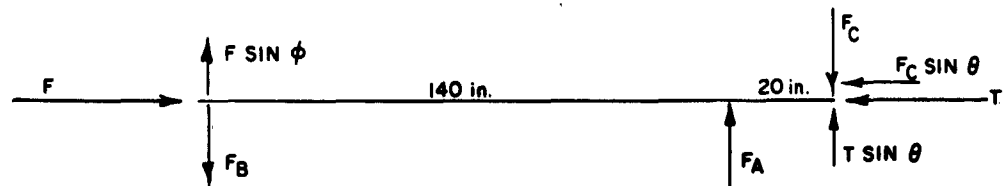
Thrust Member

In a similar way, the length of the main-thrust column that will allow the lateral load cells to be read within 0.1% accuracy can be determined. Assuming the same forces on the rocket motor as in the previous calculation and letting the lateral natural frequency of the stand be 30 cps, the lateral deflections due to F_C will be

$$\begin{array}{ll} \text{Member A, } \delta_A = 0.0075 \text{ in.} & \text{so, } \theta = 0^\circ - 00' - 15'' \\ \text{Member B, } \delta_B = 0.0019 \text{ in.} & \phi \text{ and } L \text{ are unknown} \end{array}$$



Assuming cosine functions as unity, since the errors they produce are negligibly small in this example, we have the following simplified force system:



The forces $F \sin \phi$ and $T \sin \theta$ produce error in the load cell readings F_A and F_B . Therefore, since the side force F_C is determined by the sum of the readings of these two load cells and they will be in error by an amount equal to the sum of $T \sin \theta$ and $F \sin \phi$, it is necessary to reduce these factors by making ϕ and θ small enough to be within the desired accuracy. Since θ is already determined from the assumed geometry and stiffness of the side members, the magnitude of ϕ can be calculated; from this L can be determined.

$F_C = 10,000$ lb 0.1% of this force is 10 lb. This then is the amount the sum of F_A and F_B will be allowed to be in error.

$$T \sin \theta = 100,000 (0.000067) = 6.7 \text{ lb}$$

$$\text{Then } F \sin \phi \text{ must be not more than } 10 - 6.7 = \underline{3.3 \text{ lb}}$$

$$F = 100,007 \text{ lb}$$

$$F \sin \phi = 100,007 \sin \phi = 3.3$$

$$\sin \phi = 0.000033 \quad (\phi = 0^\circ - 00' - 06'') \text{ and } \sin \phi = \frac{\delta_B}{L}$$

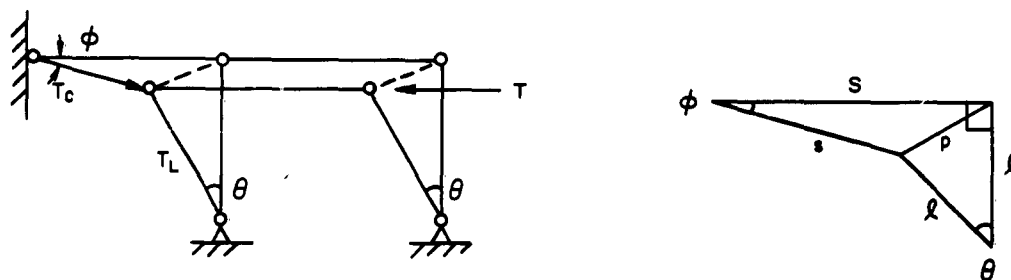
$$\text{So, } L = \frac{0.0019}{0.000033} = \underline{57.6 \text{ inches long}}$$

These calculations are based on the assumption that the stand is perfectly aligned initially. Any misalignment between motor and thrust will degrade the accuracy of the side force measurements beyond the 0.1% goal.

Appendix C

FOUR BAR LINKAGE ANALYSIS

Assuming spring constant K in thrust takeout member S only and frictionless joints.



S = unstressed length of thrust takeout
 T_C = load cell readout-lb
 T = true thrust
 l = length of legs (does not change)
 $[T_C = K(S-s) \text{ where } K \text{ is the spring constant of the thrust takeout}]$
 s = length of S under force T_C

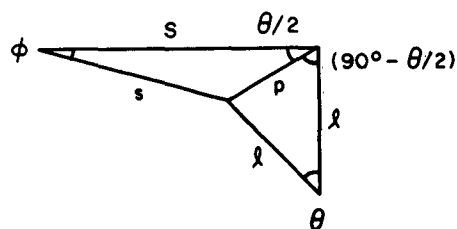
$$p^2 = S^2 + s^2 - 2Ss \cos \phi \quad (1)$$

$$p = 2l \sin \frac{\theta}{2} \quad (2)$$

combining (1) and (2):

$$4l^2 \sin^2 \frac{\theta}{2} = S^2 + s^2 - 2Ss \cos \phi$$

$$2l^2 (1 - \cos \theta) = S^2 + s^2 - 2Ss \cos \phi \quad (3)$$



$$\frac{p}{\sin \phi} = \frac{s}{\sin \frac{\theta}{2}} \quad (4)$$

$$\frac{p}{\sin \theta} = \frac{l}{\sin (90^\circ - \frac{\theta}{2})} = \frac{l}{\cos \frac{\theta}{2}} \quad (5)$$

Eliminating p from (4) and (5) and using $\tan \frac{\theta}{2} = \frac{1 - \cos \theta}{\sin \theta}$

$$\frac{s \sin \phi}{l \sin \theta} = \frac{\sin \frac{\theta}{2}}{\cos \frac{\theta}{2}} = \frac{1 - \cos \theta}{\sin \theta} \quad (6)$$

$$(1 - \cos \theta) = \frac{s}{l} \sin \phi$$

Now eliminate $(1 - \cos \theta)$ from equations (3) and (6).

$$2 l s \sin \phi = S^2 + s^2 - 2 S s \cos \phi$$

$$\cos \phi = \frac{S^2 + s^2}{2 S s} - \frac{l}{S} \sin \phi$$

Now since $T_C = K (S - s)$; $s = S - \frac{T_C}{K}$

$$\cos \phi = \frac{1 - \left(\frac{T_C}{KS}\right) + \frac{1}{2} \left(\frac{T_C}{KS}\right)^2}{\left[1 - \left(\frac{T_C}{KS}\right)\right]} - \frac{l}{S} \sin \phi$$

$$\cos \phi = A - \frac{l}{S} \sin \phi \quad \text{where } A = \frac{\left[1 - \left(\frac{T_C}{KS}\right) + \frac{1}{2} \left(\frac{T_C}{KS}\right)^2\right]}{\left[1 - \left(\frac{T_C}{KS}\right)\right]}$$

$$\cos^2 \phi + \sin^2 \phi = A^2 - 2 A \frac{l}{S} \sin \phi + \left[\left(\frac{l}{S}\right)^2 + 1\right] \sin^2 \phi$$

$$\sin \phi = \frac{\frac{A l}{S} \pm \sqrt{1 + \left(\frac{l}{S}\right)^2 - A^2}}{\left[\left(\frac{l}{S}\right)^2 + 1\right]}$$

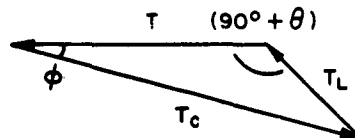
and finally;

$$\sin \phi = \frac{\left(\frac{l}{S}\right) (1 + B) \pm \sqrt{\left(\frac{l}{S}\right)^2 - (2B + B^2)}}{\left[\left(\frac{l}{S}\right)^2 + 1\right]} \quad (7)$$

$$\text{where } B = \frac{\frac{1}{2} \left(\frac{T_C}{KS}\right)^2}{\left(1 - \frac{T_C}{KS}\right)}$$

Now utilizing the force vectors \vec{T} , \vec{T}_L , \vec{T}_C :

$$\vec{T} = \vec{T}_C + \vec{T}_L$$



$$T_L^2 = T^2 + T_C^2 - 2 T T_C \cos \phi \quad (8)$$

Now by virtue of the force triangle:

$$\frac{T_L}{\sin \phi} = \frac{T_C}{\sin (90^\circ + \theta)} = \frac{T_C}{\cos \theta}$$

$$T_L = T_C \frac{\sin \phi}{\cos \theta} \quad (9)$$

Now solve (8) for T:

$$T^2 - (2 T_C \cos \phi) T + (T_C^2 - T_L^2) = 0$$

$$T = \frac{2 T_C \cos \phi \pm \sqrt{(2 T_C \cos \phi)^2 - 4 (T_C^2 - T_L^2)}}{2}$$

$$T = T_C \cos \phi \pm \sqrt{(T_C \cos \phi)^2 - (T_C^2 - T_L^2)}$$

Now plug in $T_L = T_C \frac{\sin \phi}{\cos \theta}$ [equation (9)].

$$T = T_C \cos \phi \pm T_C \sqrt{\cos^2 \phi - \left(1 - \frac{\sin^2 \phi}{\cos^2 \theta}\right)}$$

$$T = T_C \left[\cos \phi \pm \sqrt{\cos^2 \phi - 1 + \frac{\sin^2 \phi}{\cos^2 \theta}} \right]$$

$$\sin^2 \phi + \cos^2 \phi = 1$$

$$\cos^2 \phi - 1 = -\sin^2 \phi$$

$$T = T_C \left[\cos \phi \pm \sin \phi \sqrt{\frac{1}{\cos^2 \theta} - 1} \right]$$

$$T = T_C \left[\cos \phi \pm \sin \phi \tan \theta \right]$$

$$(\% \text{ error in thrust read out } T_C) = 100 \left(\frac{T_C - T}{T} \right)$$

$$\% \text{ error in } T_C = 100 \left[\frac{1}{\cos \phi \pm \sin \phi \tan \theta} - 1 \right] \quad (10)$$

$$\text{where } \phi = \sin^{-1} \left\{ \frac{\left(\frac{l}{S} \right) (1 + B) \pm \sqrt{\left(\frac{l}{S} \right)^2 - (2B + B^2)}}{\left[\left(\frac{l}{S} \right)^2 + 1 \right]} \right\}$$

$$\text{wherein } B = \frac{1}{2} \left(\frac{T_C}{KS} \right)^2$$

$$\left[1 - \left(\frac{T_C}{KS} \right) \right]$$

$$\text{and } \theta = \cos^{-1} \left\{ 1 - \left[\frac{1 - \left(\frac{T_C}{KS} \right)}{\left(\frac{l}{S} \right)} \right] \sin \phi \right\}$$

θ is derived by virtue of equation (6) and $T_C = K(S-s)$ in a manipulation as follows:

$$\begin{aligned} \text{Equation (6)} \quad (1 - \cos \theta) &= \frac{s}{l} \sin \phi \\ \cos \theta &= 1 - \frac{s}{l} \sin \phi \\ \cos \theta &= 1 - \frac{1}{l} \left(S - \frac{T_C}{K} \right) \sin \phi \\ \theta &= \cos^{-1} \left[1 - \frac{1}{l} \left(S - \frac{T_C}{K} \right) \sin \phi \right] \\ \theta &= \cos^{-1} \left[1 - \frac{\left(1 - \frac{T_C}{KS} \right) \sin \phi}{\frac{l}{S}} \right] \end{aligned}$$

Now utilizing a measured $K = 429,000$ lb/in and $S = 112$ in, $l = 53$ in, and $T_C = 100,000$ lb.

$$(S - s) = \frac{T_C}{K} = \frac{10^5}{4.29 \times 10^5} = 0.233 \text{ in. deflection under steady state thrust.}$$

$$\frac{T_C}{KS} = 2.081 \times 10^{-3} \text{ dimensionless}$$

$$\left. \begin{array}{l} \phi = 0^\circ 0' 0.947'' \\ \theta = 0^\circ 15' 7.68'' \end{array} \right\} \begin{array}{l} \text{angular} \\ \text{deflections under steady} \\ \text{state thrust } T = 10^5 \text{ lb} \end{array}$$

% error in $T_C = 0.0000021\%$ negligible for this case of perfect alignment.

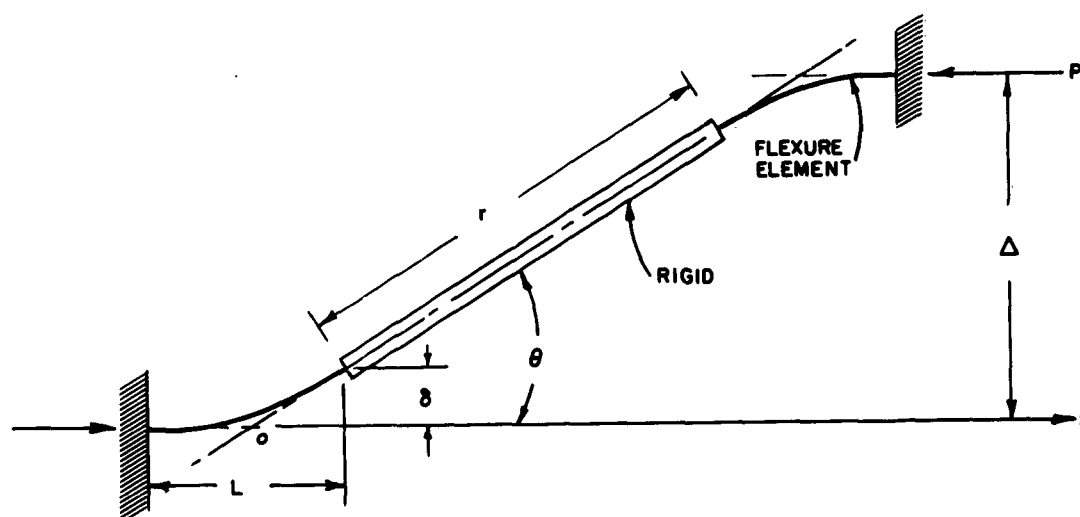
$$T_L = T_C \frac{\sin \phi}{\cos \theta} = 10^5 \frac{\sin 0^\circ 0' 0.947''}{\cos 0^\circ 15' 7.68''}$$

$$T_L = \frac{0.4592412}{0.999903155} = \underline{0.459 \text{ lb}} \quad \begin{array}{l} \text{Reading in front leg} \\ \text{load cell} \end{array}$$

Appendix D

FLEXURE ANALYSIS

Consider a typical flexured stand member loaded in compression by load P and deflected a distance Δ .



Assuming that point O is at $x = L/2$, then $\Delta = 2\delta + r \sin\theta$ and for small angles ($\theta < 1^\circ$), let $\sin\theta = \theta$, so

$$\Delta \cong 2\delta + r\theta \quad (1)$$

Also $\theta = \tan^{-1} \frac{\Delta}{r\cos\theta + L}$ and letting $\tan\theta = \theta$ and $r \cos\theta \cong r$

$$\theta \cong \frac{\Delta}{r+L} \quad (2)$$

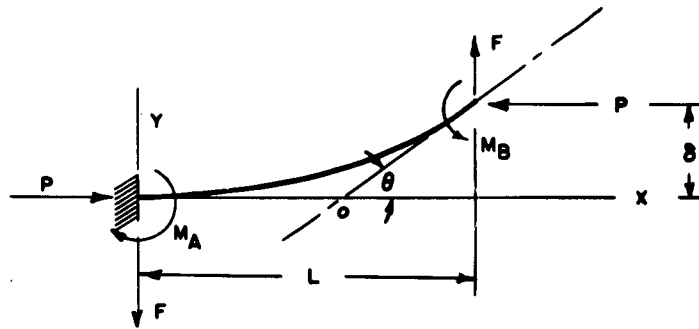
Combining Eqs. 1 and 2 we have:

$$\delta = \frac{L\Delta}{2(r+L)} \quad (3)$$

This approximation is accurate to within a few percent for θ up to 1° .

The unknowns now are F and M , the resisting forces due to the bending of the flexure elements.

Consider one flexure element with the forces acting on it as shown.



The equation for the deflection curve of the flexure element above is:

$$EI \frac{d^2 y}{dx^2} = M \quad (4)$$

where M is the bending moment in the element due to the forces applied to it. Summing these moments we obtain:

$$\begin{aligned} EI \frac{d^2 y}{dx^2} &= -Py + M_A - Fx \\ \frac{d^2 y}{dx^2} + \frac{P}{EI} y &= \frac{M_A}{EI} - \frac{F}{EI} x \end{aligned} \quad (5)$$

introducing the operator $D = \frac{dy}{dx}$; $D^2 = \frac{d^2 y}{dx^2}$

$$D^2 + \frac{P}{EI} y = \frac{M_A}{EI} - \frac{F}{EI} x \quad (6)$$

The solution of this differential equation embodies the complementary function plus the particular solution, or:

$$y = y_c + y_p$$

The complementary function is:

$$D^2 + \frac{P}{EI} y = 0$$

The auxiliary roots are,

$$D = \pm i \sqrt{\frac{P}{EI}}$$

This equation has a solution in the form:

$$y_c = Ae^{i\sqrt{\frac{P}{EI}}x} + Be^{-i\sqrt{\frac{P}{EI}}x} \quad (7)$$

which can be written as:

$$y_c = Q \sin \beta x + R \cos \beta x \quad (8)$$

$$\text{where } \beta = \sqrt{\frac{P}{EI}}.$$

The particular solution of Eq. 6 is:

$$y_p = \frac{EI}{P} \left(\frac{M_A}{EI} - \frac{F}{EI} x \right) = \frac{1}{P} (M_A - Fx) \quad (9)$$

The general solution for Eq. 6 is then:

$$y = Q \sin \beta x + R \cos \beta x + \frac{1}{P} (M_A - Fx) \quad (10)$$

Now, when $x = 0$, $y = 0$ and $R = -\frac{M_A}{P}$

$$\frac{dy}{dx} = Q\beta \cos \beta x - R\beta \sin \beta x - \frac{F}{P}$$

When $x = 0$, $\frac{dy}{dx} = 0$ and $Q = \frac{F}{P\beta}$.

Substituting these values R and Q into Eq. 10 we have:

$$y = \frac{F}{P\beta} \sin \beta x - \frac{M_A}{P} \cos \beta x + \frac{1}{P} (M_A - Fx) \quad (11)$$

This is the equation describing the bent flexure element.

Useful equations involving the flexure parameters, length, and deflection can be obtained from Eq. 11 by the substitutions $x = L$ and $y = \delta$ and $\frac{dy}{dx} = \theta$ when $x = L$.

$$\frac{dy}{dx} = \frac{F}{P} \cos \beta x + \frac{M_A}{P} \beta \sin \beta x - \frac{F}{P} \quad (12)$$

and substituting $L = x$, $\delta = y$ and $\theta = \frac{dy}{dx}$ we have:

$$\delta = \frac{F}{P\beta} \sin \beta L - \frac{M_A}{P} \cos \beta L + \frac{1}{P} (M_A - FL) \quad (13)$$

$$\theta = \frac{F}{P} \cos \beta L + \frac{M_A}{P} \beta \sin \beta L - \frac{F}{P} \quad (14)$$

where $\beta = \sqrt{\frac{P}{EI}}$.

Generally, δ , θ , and P are known and M_A and F are to be found. Equations 13 and 14 are now solved for M_A and F , respectively.

$$M_A = \frac{FL + P\delta - \frac{F}{\beta} \sin \beta L}{(1 - \cos \beta L)} \quad (15)$$

$$F = \frac{M_A \beta \sin \beta L - P\theta}{(1 - \cos \beta L)} \quad (16)$$

NOTE: These equations are valid only for a flexure element in compression. For an element in tension Eq. 5 must be evaluated with $-P = P$. In this case, the complementary function no longer has imaginary roots and the general solution will have a different form.

For P causing tension, Eq. 5 becomes:

$$EI \frac{d^2 y}{dx^2} = Py + M_A - Fx \quad (17)$$

Following the same procedure as before, the complementary solution now has the form:

$$y_c = Ae^{\beta x} + Be^{-\beta x}$$

or,

$$y_c = Q \sinh \beta x + R \cosh \beta x \quad (18)$$

and the general solution is:

$$y = Q \sinh \beta x + R \cosh \beta x + \frac{1}{P} (M_A - Fx) \quad (19)$$

The equation in terms of δ , θ , M_A and F are:

$$\delta = \frac{F}{P\beta} \sinh \beta L - \frac{M_A}{P} \cosh \beta L + \frac{1}{P} (M_A - FL) \quad (20)$$

$$\theta = \frac{F}{P} \cosh \beta L - \frac{M_A}{P} \beta \sinh \beta L - \frac{F}{P} \quad (21)$$

$$M_A = \frac{FL + P\delta - \frac{F}{\beta} \sinh \beta L}{(1 - \cosh \beta L)} \quad (22)$$

$$F = \frac{M_A \beta \sinh \beta L + P\theta}{(\cosh \beta L - 1)} \quad (23)$$

REFERENCES

1. Faires, V. M. Design of Machine Elements, 3rd ed. New York, MacMillan, 1955. P. 323.
2. Ormond, A. N. "Flexures Used in Force and Thrust Measuring Systems", Fall Instrument-Automation Conference and Exhibit, Los Angeles, California, September 11-15, 1961, INST SOC AM, Preprint Number 118-LA61.
3. U. S. Naval Ordnance Test Station. A System for Correction for Spurious Natural Frequency Ringing of Rocket Static Thrust Stands, by John S. Ward. China Lake, Calif., NOTS, 1 September 1960. (NAWWEPS Report 7569, NOTS TP 2541).
4. -----. Description of a Control System for Rocket-Motor Mass Measurement, by R. A. Elston. China Lake, Calif., NOTS, June 1963. (NAWWEPS Report 8354, NOTS TP 3241).
5. -----. Determination of Rocket-Motor Mass by Measurement of the Natural Frequency of a Mass-Spring System, by Benjamin Glatt. China Lake, Calif., NOTS, 15 June 1961. (NAWWEPS Report 7741, NOTS TP 2706).
6. Wittrick, W. H. "The Properties of Crossed Flexures Pivots and the Influence of the Point at Which the Strips Cross", THE AERONAUTICAL QUARTERLY, Vol. II (February 1951), pp. 272-292.

INITIAL DISTRIBUTION

- 9 Chief, Bureau of Naval Weapons
 - FWAM (1)
 - R-14 (1)
 - RM-3 (1)
 - RM-35 (1)
 - RMMP (1)
 - RMMP-12 (1)
 - RMMP-241 (1)
 - RMMP-4 (1)
 - RT (1)
- 10 Special Projects Office
 - Sp-00 (1)
 - Sp-01 (1)
 - Sp-20 (1)
 - Sp-27 (1)
 - Sp-271 (3)
 - Sp-274 (2)
 - Sp-3 (1)
- 4 Chief of Naval Operations (Operations Evaluation Group)
- 1 Chief of Naval Research (Code 104)
- 1 Naval Air Test Center, Patuxent River (Aeronautical Publications Library)
- 1 Naval Avionics Facility, Indianapolis (Library)
- 1 Naval Explosive Ordnance Disposal Facility, Naval Propellant Plant, Indian Head
- 1 Naval Propellant Plant, Indian Head
- 1 Naval Weapons Evaluation Facility, Kirtland Air Force Base (Code 401)
- 2 Naval Weapons Services Office
 - 1 Operational Test and Evaluation Force
- 2 Bureau of Naval Weapons Branch Representative, Cumberland (SPH)
- 1 Bureau of Naval Weapons Representative, Azusa
- 3 Bureau of Naval Weapons Representative, Sunnyvale (SPL)
- 2 Bureau of Naval Weapons Resident Representative, Bacchus (SPLB)
- 2 Bureau of Naval Weapons Resident Representative, Sacramento (SPLA)
- 1 Picatinny Arsenal
- 1 Air Force Cambridge Research Laboratories, Laurence G. Hanscom Field
- 1 Air Force Flight Test Center, Edwards Air Force Base
- 1 Air Proving Ground Center, Eglin Air Force Base
- 1 Arnold Engineering Development Center, Tullahoma
- 2 National Aeronautics and Space Administration
 - R.Ziem (1)
 - W.Cohen (1)
- 1 Allegany Ballistics Laboratory, Cumberland
- 1 Applied Physics Laboratory, JHU, Silver Spring

ABSTRACT CARD

<p>U. S. Naval Ordnance Test Station</p> <p><u>Design Criteria for Large Accurate Solid-Propellant Static-Thrust Stands</u>, by D. P. Ankeney and C. E. Woods. China Lake, Calif., NOTS, June 1963. 48 pp. (NAWEPs Report 8353, NOTS TP 3240), UNCLASSIFIED.</p> <p>ABSTRACT. This report presents design criteria for the construction of a large solid-propellant static-thrust stand to meet specific requirements of accuracy, flexibility, adaptability, ease of assembly and operation, safety, and low cost. Design concepts of dynamic stand evaluation, calibration accuracy and</p> <p style="text-align: right;">(Over) 1 card, 4 copies</p>	<p>U. S. Naval Ordnance Test Station</p> <p><u>Design Criteria for Large Accurate Solid-Propellant Static-Thrust Stands</u>, by D. P. Ankeney and C. E. Woods. China Lake, Calif., NOTS, June 1963. 48 pp. (NAWEPs Report 8353, NOTS TP 3240), UNCLASSIFIED.</p> <p>ABSTRACT. This report presents design criteria for the construction of a large solid-propellant static-thrust stand to meet specific requirements of accuracy, flexibility, adaptability, ease of assembly and operation, safety, and low cost. Design concepts of dynamic stand evaluation, calibration accuracy and</p> <p style="text-align: right;">(Over) 1 card, 4 copies</p>
<p>U. S. Naval Ordnance Test Station</p> <p><u>Design Criteria for Large Accurate Solid-Propellant Static-Thrust Stands</u>, by D. P. Ankeney and C. E. Woods. China Lake, Calif., NOTS, June 1963. 48 pp. (NAWEPs Report 8353, NOTS TP 3240), UNCLASSIFIED.</p> <p>ABSTRACT. This report presents design criteria for the construction of a large solid-propellant static-thrust stand to meet specific requirements of accuracy, flexibility, adaptability, ease of assembly and operation, safety, and low cost. Design concepts of dynamic stand evaluation, calibration accuracy and</p> <p style="text-align: right;">(Over) 1 card, 4 copies</p>	<p>U. S. Naval Ordnance Test Station</p> <p><u>Design Criteria for Large Accurate Solid-Propellant Static-Thrust Stands</u>, by D. P. Ankeney and C. E. Woods. China Lake, Calif., NOTS, June 1963. 48 pp. (NAWEPs Report 8353, NOTS TP 3240), UNCLASSIFIED.</p> <p>ABSTRACT. This report presents design criteria for the construction of a large solid-propellant static-thrust stand to meet specific requirements of accuracy, flexibility, adaptability, ease of assembly and operation, safety, and low cost. Design concepts of dynamic stand evaluation, calibration accuracy and</p> <p style="text-align: right;">(Over) 1 card, 4 copies</p>

NAWEPs REPORT 8353

error analysis, continuous-mass measurement, in-place calibration, alignment, damage control, and environmental testing are discussed. Also included in the report is a suggested design procedure formulated to provide guidance in the design and development of a static-test stand that will attain the unique goals of a particular facility. This report supersedes IDP 1551 of the same title, dated December 1962.

NAWEPs REPORT 8353

error analysis, continuous-mass measurement, in-place calibration, alignment, damage control, and environmental testing are discussed. Also included in the report is a suggested design procedure formulated to provide guidance in the design and development of a static-test stand that will attain the unique goals of a particular facility. This report supersedes IDP 1551 of the same title, dated December 1962.

NAWEPs REPORT 8353

error analysis, continuous-mass measurement, in-place calibration, alignment, damage control, and environmental testing are discussed. Also included in the report is a suggested design procedure formulated to provide guidance in the design and development of a static-test stand that will attain the unique goals of a particular facility. This report supersedes IDP 1551 of the same title, dated December 1962.

NAWEPs REPORT 8353

error analysis, continuous-mass measurement, in-place calibration, alignment, damage control, and environmental testing are discussed. Also included in the report is a suggested design procedure formulated to provide guidance in the design and development of a static-test stand that will attain the unique goals of a particular facility. This report supersedes IDP 1551 of the same title, dated December 1962.

- 1 Bruce H. Sage Consultant, Pasadena
- 1 Hercules Powder Company, Bacchus Works, Bacchus, Utah
- 1 Inca Engineering Corporation, Pasadena
- 2 Lockheed Aircraft Corporation, Missiles and Space Division, Palo Alto, Calif.
- 1 Thompson Ramo Wooldridge Inc., RW Division, Canoga Park, Calif. (Technical Information Services)
- 148 Joint Army-Navy-Air Force Mailing List for the Distribution of Solid Propellant Technical Information, dated June 1962